CONSENSUS BUILDING IN SENSOR NETWORKS AND LONG TERM PLANNING FOR THE NATIONAL AIRSPACE SYSTEM

Naga Venkata Swathik Akula

Thesis Prepared for the Degree of

MASTER OF SCIENCE

UNIVERSITY OF NORTH TEXAS

May 2011

APPROVED:

Yan Wan, Major Professor
Xinrong Li, Committee Member
Miguel F. Acevedo, Committee Member
Murali Varanasi, Chair of the Department of Electrical Engineering
Costas Tsatsoulis, Dean of College of Engineering
James D. Meernik, Acting Dean of the Toulouse Graduate School

Akula, Naga Venkata Swathik. *Consensus building in sensor networks and long term planning for the National Airspace System*. Master of Science (Electrical Engineering), May 2011, 57 pp., bibliography, 36 titles.

In this thesis, I present my study on the impact of multi-group network structure on the performance of consensus building strategies, and the preliminary mathematical formulation of the problem on improving the performance of the National Airspace system (NAS) through long term investment. The first part of the thesis is concerned with a structural approach to the consensus building problem in multi-group distributed sensor networks (DSNs) that can be represented by bipartite graph. Direct inference of the convergence behavior of consensus strategies from multi-group DSN structure is one of the contributions of this thesis. The insights gained from the analysis facilitate the design and development of DSNs that meet specific performance criteria. The other part of the thesis is concerned with long-term planning and development of the NAS at a network level, by formulating the planning problem as a resource allocation problem for a flow network. The network-level model viewpoint on NAS planning and development will give insight to the structure of future NAS and will allow evaluation of various paradigms for the planning problem.

Copyright 2011

By

Naga Venkata Swathik Akula

ACKNOWLEDGMENTS

I would like to express my gratitude to my advisor, Dr.Yan Wan for her guidance and support. Her motivation really helped me to complete my tasks and achieve the results. I would like to thank Dr.Xinrong Li and Dr.Miguel F.Acevedo for their support as committee members of my thesis. I am grateful for the support of my friend Sreenika during my writings. Lastly, I thank my parents and sister for their encouragement towards my interests, and making my every success truly memorable.

CONTENTS

CHAPTER 1

INTRODUCTION

This thesis is divided in two parts: 1)the impact of multi-group network structure on the performance of consensus building strategies (the journal version was submitted [2]), and 2)the preliminary mathematical formulation for improving the performance of the National Airspace System (NAS) through long-term investment.

Consensus building refers to the process in which each sensor node starting with its initial estimate about a parameter of interest, arrives at a common value through a localized iterative updating process. Hierarchical multi-group structure is common to distributed sensor networks (DSN) in many natural and engineering applications. Although network structure plays a crucial role in the performance of consensus building strategies in such networks, little work has been done to establish the precise connection between the two. In this thesis, a structural approach is considered to the consensus building problem in multi-group DSN that can be described by bipartite graphs. Specifically, for a typical iterative averaging consensus algorithm defined on such DSNs, the eigen-structure is associated with the dynamics of the iterative process, and the eigen-structure is related to simple characteristics of the network connectivity pattern. The exact conditions for consensus are established and a precise relationship between the consensus value and the degree distribution of the nodes in the bipartite graph is derived. Direct inference of the convergence behavior of consensus strategies from DSN structure is one of the contributions of this thesis. The insights gained from the analysis facilitate the design and development of DSNs that meet specific performance requirements.

The other part of the thesis is concerned with long-term planning and development of the NAS. During the next few decades, the NAS will substantially increase in complexity, with

ever-growing and changing traffic demand, more congestion concerns, novel paradigms for traffic control and flow management, among many other factors. The increasing complexity makes long term planning of the NAS both important and challenging. Specifically, the long-term planning of the NAS is considered at a network level, by formulating the planning problem as a resource allocation problem for a flow network. Specifically, a preliminary network model is constructed for flows that transit among airports in the NAS, and an optimization problem is formulated which is aimed to minimize the total delay in the NAS over a time span with limited infrastructure delivery cost and increasing traffic demand. An example is constructed that shows the use of model for comparison of different planning schemes. The network-level viewpoint on NAS planning and development will give further insight of future NAS and will allow comparison, evaluation, and refinement of various paradigms for the planning problem.

CHAPTER 2

CONSENSUS BUILDING IN MULTI-GROUP SENSOR NETWORKS

2.1. Background and Problem Formulation for Consensus Building

2.1.1. Introduction

Consensus problem widely appears in natural and engineering applications, and has received extensive study (see e.g., [9–11, 13, 15]). However, it has not been investigated much in the context of multi-group structures; i.e., networks composed of multiple groups, in each of which some nodes are designated as leaders and given the responsibility of communicating with other groups. Such hierarchical multi-group structure is commonly observed in nature and has great potential for engineered systems. For instance, hierarchical group structure is typically observed in bird flocking as studied in e.g., [6]. Similarly, in Distributed Sensor Networks (DSN), properly designed hierarchical communication structure has the potential to be more energy efficient due to the function separation of sensors and the organized routing structures [1].

The potential applications of employing networks of agents to arrive at a common value are discussed in many fields. In multi- vehicle cooperative control, large numbers of autonomous vehicles (air, ground and water) are envisioned to have a significant impact in civilian and homeland security applications (e.g., monitoring forest fires, old fields, pipelines, tracking wild fire, monitoring the perimeter of nuclear power plants). To enable these applications the agents coordinate with each other. For sensor network applications, such as mobile target tracking, event detection, it is essential that the nodes act in a coordinated and synchronized fashion. In all of these application areas, inferring convergence behavior of consensus building strategies is the study of interest.

Network structure has known to be crucial to the performance of consensus building [15]. In designing multi-group network structures for consensus building, one question is whether there exists a quantitative relationship between the network structure and its performance, especially in large-scale networks, where scalability is important. In this thesis, this issue was addressed by studying the network design problem for some common hierarchical multi-group structures. In order to represent the information flow in a multi-group DSN, it is beneficial to describe a DSN using an equivalent graphical model that can abstract and capture its connectivity patterns. Examples of some graphical models are illustrated in figure 2.1.

In this thesis, the focus is on the bipartite graph structure (figure 2.1a) which is widely used in communications and has been recently adopted for sensor network applications [3, 19]. The objective is to investigate the effect of network structure on the convergence behavior of consensus building strategies. Specifically, a structural approach is considered to study the research questions of interest in consensus building, including whether consensus can be reached by the network, what is the final consensus value, and how many iterations are needed to reach the consensus. Direct inference of the convergence behavior of the consensus strategies from DSN structures is one of the contributions of this thesis. These results in turn, lead to efficient and scalable strategies for designing DSNs (e.g., the selection of the number of leaders and network connections) to meet desirable performance requirements. It is worthwhile to note that the structural approach also suggests a way to investigate algebraic graph-theory related aspects by working with indirect graphs rather than the graph directly associated with network dynamics. This approach can expose some hidden features of graph structures and provide insightful analytical results on network dynamics that are not possible otherwise.

Further, in section 2.1.2, the research problem is formulated, and in section 2.1.3, a brief review of relevant literature is provided. The section 2.2 provides the condition for reaching consensus and the consensus value that all sensor nodes finally agree to. The section 2.3,

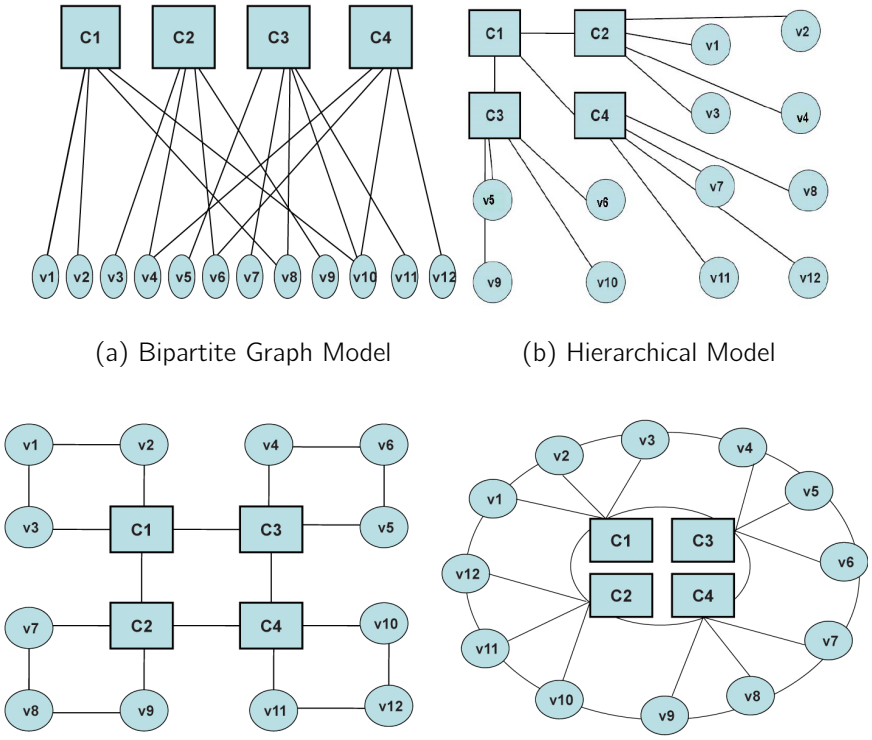

(a) Bipartite Graph Model (b) Hierarchical Model

(c) Mesh Model (d) Semi-regular Graph Model

Figure 2.1. Four sample networks, each consisting of 16 nodes (twelve member nodes V1 to V12, and four leader nodes, C1 to C4) forming four groups, are shown here. In each group, one node serves as the leader. Information flows in both directions i.e., from the agents to the leaders and from the leaders to the agents.

explores the estimation of convergence time through eigen-analysis, and the relationship between network structure and the performance of the consensus strategy for subclasses of connectivity patterns.

2.1.2. Problem Formulation

Consensus building refers to the process in which each sensor node starting with its initial estimate about a parameter of interest, arrives at a common value, through a localized iterative

updating process. In each iteration, each node updates its estimate based on the information received from its neighbors and then shares its updated estimate with its neighbors. In a network structure, each sensor node has the same functionality with respect to sensing and information processing. However, in each group, some sensor nodes are designated as leaders or fusion centers. To facilitate the analysis, the sensing functionality is removed from fusion centers, and the concept of virtual fusion centers (VFCs) are introduced, whose responsibilities are solely on establishing connections within and between the groups (as shown in figure 2.2). The VFCs are represented by square nodes, sensors are represented by circles, and communication links are represented by edges. The functionality of a VFC can be implemented at any node as shown in the figure on the right. This representation is not limited to a small number of nodes. It can be applied to more complex and general network structures.

The main focus is on networks whose structure can be represented by a bipartite graph as shown in figure 2.1(a) (see [3] for a detailed description). Bipartite graphs, are also known as tanner graphs [7], in coding theory. The network structure of a tanner graph is represented by its parity matrix. Here, the parity matrix is referred as routing matrix in the context of a DSN. Assuming that a DSN has m VFCs and n sensor nodes, its structure can be captured by a $m \times n$ routing matrix H, in which the entry in (i, j) is set to "1" if there is communication link between the i^{th} VFC and the j^{th} sensor node. If the degrees (i.e., the number of communication links) of all VFC nodes are the same, then the DSN is said to be regular.

The motivation for the consensus building strategy comes from the belief propagation (BP) concepts developed by Gallager in 1963 [19] with applications to channel coding and Pearl's algorithm developed in 1980s by the artificial intelligence community. It begins with the sensors observing a common phenomenon by taking their own measurements. In each iteration, each VFC receives inputs from the sensors connected to it, aggregates the information, and then updates all the sensor nodes with the new value it computed. The iterative algorithm

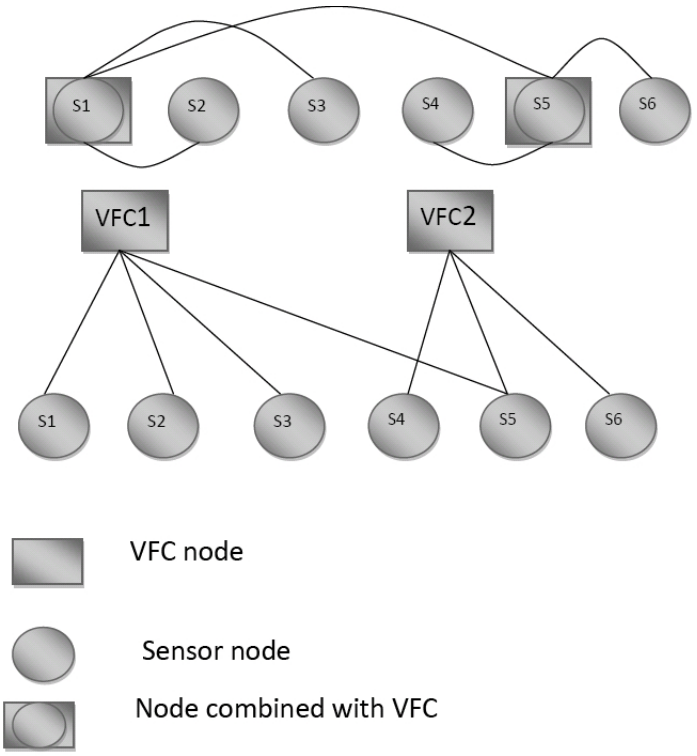

Figure 2.2. An example of DSN and its tanner graph representation

converges to a final value and the consensus is reached by all nodes at the same time. Each iteration in the consensus building process consists of two operations.

1) Forward operation: In the first half of the iteration, each sensor sends its own value to the VFC to which it is connected.

2) Backward operation: In the second half of the iteration, each VFC updates the sensor nodes with its new result. A VFC may employ a linear or a non-linear process to aggregate its input based on factors such as the type and proximity of the sensor to the target. Here, the collected values from all connected sensor nodes are assumed to be aggregated by a simple averaging operation based on the number of sensors it is receiving information from. In another words, each VFC calculates the average of all observations it received and sends this new estimate to each sensor node that it is connected to. Each sensor node then updates its

value by taking the average of new estimates it receives from the VFCs that it is connected to. This typical consensus building algorithm is referred as the iterative averaging algorithm.

Let me illustrate the two operations involved in an iteration through an example (figure 2.3). During the forward operation, VFC1 and VFC2 receive and aggregate the values from their connected sensor nodes S1, S2, S3, S5 and S4, S5, S6 respectively by averaging them (figure 2.3a). During the backward operation(figure 2.3b), S1, S2, S3 update to the averaged value sent from VFC1, and S4, S6 update to the value sent from VFC2. S5, updates to the averaged value of VFC1 and VFC2.

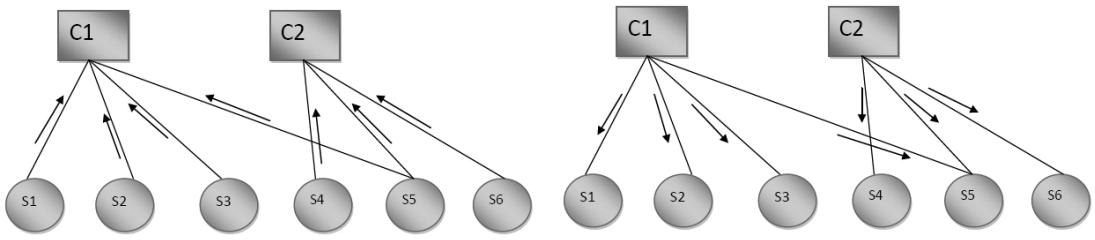

Figure 2.3. a) Forward operation; b) Backward operation

2.1.3. Background

Consensus problems have been extensively studied in a multitude of fields, including sensor networking [9–11], distributed computing [16, 18], and decentralized control [13, 15], among others. A brief review of the most relevant literature is provided with the aim to motivate the approach.

In a closely related work, Boyd et. al. studied the convergence condition and convergence time for a network of autonomous sensors [9, 10]. The authors formulate the design of network structure for fast convergence as an optimization problem and use the semi-definite programming approach to solve it numerically. The work in this thesis is different from theirs in mainly three ways. First, my study is on multi-group DSNs that have inherent structures rather than a network of egalitarian sensor nodes without any group structure. Second, works

[9, 10] consider the final consensus value as an average of all sensor nodes' initial values. In reality, sensor nodes may contribute unequally to the final consensus value, hence the contribution of each sensor to the consensus value is allowed to be free design variable. Finally, an explicit and closed-form relationship between the network structure and its convergence behavior is derived, rather than providing a numerical approach.

Consensus problems have received huge attention from the decentralized control community, whose focus is mainly on building local controllers to achieve consensus among agents. The works in this field are to some extent originated from [12]. A tutorial paper [13] provides an overview of the literature in this domain for networks with first-order dynamics and Laplacian topology. Also of particular relevance to my approach is [15] which presents some intersting results about the dependence of the consensus value on initial conditions and network topology.

Although in areas such as the science of networks, network structure and its impact on performance has been previously investigated, there has been very limited research in evaluating the impact in a quantitative manner, and in network design for consensus strategies that exploit network structure. Some of the relevant research is summarized here. A common optimal scaling problem for networks was investigated in [23]. A design that gives structural insights for the limited resource allocation problem was given in [22]. For networks with tree structures, a structural approach to weight assignment to edges in such a way to maximize the algebraic connectivity was explored in [20, 21].

Algebraic graph theory provides very useful insights into network design, due to the ability of eigen-analysis in connecting network structures and the dynamics. Examples of the results in this field can be found in [8].

From the above literature review, it can be observed that despite the existence of abundant literature on consensus building and the realization that network connectivity structure plays a crucial role in the performance of consensus building strategies, there is very limited effort on directly relating network structure to the performance of consensus building strategies and the

design of network connectivity patterns for consensus building. The goal is to bridge this gap, and investigate the tanner graph representation of multiple-group DSN, and show that the consensus condition, the final consensus value, and performance of consensus building can be directly inferred from the network structure for broad classes of network topologies. These results allow to explicitly design DSNs with connectivity patterns that meet the desirable performance specifications without using complicated numerical computations.

2.2. Condition for Convergence and its Final Value

This section provides the impact of network structure on condition for convergence and its final value for the multi-group DSN model and the iterative averaging algorithm formulated in section 2.1.2. Here the dynamics of the system are discussed along with general conditions for convergence. The derived results directly relate convergence time with DSN structure and provide insights into the design of DSNs.

In order to analyze the convergence behavior of consensus strategies, first obtain the dynamics of sensor values, and then analyze the asymptotic behavior of these dynamics. In order to do that, a vector $x[k] \in R^{n\times 1}$ is introduced to hold the values of all sensor nodes at cycle k. Recall in section 2.1.2 that during each cycle, two operations are involved: the forward and backward operations. According to the iterative averaging algorithm, after the forward operation, the values held at the VFCs are found to be $y[k+1] = K_2 H x[k]$, where the $m \times m$ diagonal matrix $K_2 = [diag(H1_{n\times 1})]^{-1}$. Here, diag() represents the operation that places the vector in the parenthesis onto the main diagonal. For instance, $diag(1_{n\times 1})$ is a $n \times n$ identity matrix. Similarly, the values at the sensors after the backward operation can be computed using $x[k+1] = K_1 H^T y[k+1]$, where the $n \times n$ diagonal matrix $K_1 = [diag(H^T 1_{m\times 1})]^{-1}$. The effect of the two operations in one cycle can be captured by the following linear time-invariant (LTI) difference equation:

$$x[k+1] = Ax[k] = K_1 H^T K_2 H x[k], \tag{2.2.1}$$

where A is used to describe the system matrix. The eigenvalues of A provide rich information into the system dynamics, and in turn on the convergence behavior of the consensus strategy. In the later section, the properities of eigen values associated with system matrix A are discussed in detail.

2.2.1. Eigen-Analysis

Eigen analysis is the way of determining the dynamic properities of the system through eigenvalues and eigenvectors. The stability and performance are the two characteristics that can be inferred from eigen analysis. For a discrete-time system, if there exists an eigenvalue greater than 1, the system is unstable. For a continous-time system, if the largest eigenvalue is positive, the system dynamics will explode exponentially; if the largest eigenvalue is negative the system dynamics will decay exponentially and if the largest eigenvalue are imaginary the system will oscillate. The approach discussed here shows that for a DSN system to be stable, there exists only one eigenvalue at 1 and all the other eigenvalues are less than 1. For such a system, the response of the difference between the sensor value and final consensus value reaches zero. If there exists more than one eigenvalue at 1, then there exists more than one final consensus value, and the difference between sensor value and final consensus value doesn't tend to zero. Based on these eigenvalues, the performance of the system such as final consensus value and convergence time can be found. The later sections provide that the dominant eigenvalue of system matrix A is λ_1 and its corresponding eigenvectors w_1^T contributes to the final consensus value and λ_2 of A gives the convergence rate of the structure. Based on λ_2 analysis, the fast convergence networks for high performance is designed.

Theorem 1: The eigenvalues of the system matrix A described in equation (2.2.1) are real, simple, and reside between 0 and 1. At least one eigenvalue is equal to 1. Moreover, the multiplicity of the eigenvalue with a value 0 is greater than or equal to $n - m$.

Proof- Now examine the properties of the system matrix A. Because the row sum of $[diag(H^T 1_{m\times 1})]^{-1}H^T$ is 1 and the row sum of $[diag(H1_{n\times 1})]^{-1}H$ is also 1, it shows that A is a stochastic matrix in the sense that the row sum of A is 1 and each entry of A is non-negative. Hence A has at least one eigenvalue at 1 with associated right eigenvector $1_{n\times 1}$.

To show that the eigenvalues of matrix A are real, simple, and non-negative, let me introduce a symmetric matrix $\hat{A} = K_1^{\frac{1}{2}} H^T K_2 H K_1^{\frac{1}{2}}$, and show that the eigenvalues of A are the same as the eigenvalues of the symmetric matrix $\hat{A}$. Supposing that w_i is a left eigenvector of A corresponding to the eigenvalue λ_i, it implies $w_i^T K_1 H^T K_2 H = w_i^T \lambda_i$. This expression can be rewritten as $w_i^T K_1^{\frac{1}{2}} K_1^{\frac{1}{2}} H^T K_2 H K_1^{\frac{1}{2}} = w_i^T K_1^{\frac{1}{2}} \lambda_i$ by multiplying $K_1^{\frac{1}{2}}$ on both sides. This equation informs that for any eigenvalue λ_i and left eigenvector w_i^T associated with A, $\hat{A} = K_1^{\frac{1}{2}} H^T K_2 H K_1^{\frac{1}{2}}$ has the same eigenvalue λ_i with the left eigenvector $w_i^T K_1^{\frac{1}{2}}$. Since eigenvalues associated with a symmetric matrix $\hat{A}$ are all real and simple, the eigenvalues of A are also real and simple. Moreover, since $\hat{A}$ is positive semi-definite, the eigenvalues of A are non-negative.

What is left to show is that the multiplicity of the eigenvalue at 0 is greater than or equal to $n - m$. This is straightforward since the multiplicity of the eigenvalue 0 equals $n - rank(A)$ and the rank of A is less than or equal to the rank of H which is at most m.

Theorem 1 shows the range of eigenvalues of the system matrix A. Since the eigenvalues are real and reside between 0 and 1, they are represented as $1 = \lambda_1 \geq \lambda_2 \geq ... \geq \lambda_n \geq 0$. Moreover, the normalized left and right eigenvectors associated with λ_i are denoted as w_i^T and v_i, respectively. Further analysis show that the eigenstructure of the system matrix A plays a crucial role in consensus building. Theorem 2, presents the necessary and sufficient condition for consensus, and theorem 3 presents the quantitative description of the dependence of consensus value on network structure captured by the routing matrix H. Now the above theorem 1 is illustrated with an example.

Example 1: Consider the structure in the figure 2.4. The routing matrix $H=\begin{bmatrix}1 & 1 & 1 & 0\\ 0 & 1 & 0 & 1\end{bmatrix}$.

$K_1= [diag(H^T 1_{m\times 1})]^{-1}= [diag(\begin{bmatrix}1 & 2 & 1 & 1\end{bmatrix})]^{-1}= \begin{bmatrix}1 & 0 & 0 & 0\\ 0 & 1/2 & 0 & 0\\ 0 & 0 & 1 & 0\\ 0 & 0 & 0 & 1\end{bmatrix}$.

and $K_2= [diag(H1_{n\times 1})]^{-1}= [diag(\begin{bmatrix}3 & 2\end{bmatrix})]^{-1}= \begin{bmatrix}1/3 & 0\\ 0 & 1/2\end{bmatrix}$.

This implies $K_1H^T= \begin{bmatrix}1 & 0\\ 1/2 & 1/2\\ 1 & 0\\ 0 & 1\end{bmatrix}$ and

$K_2H= \begin{bmatrix}1/3 & 1/3 & 1/3 & 0\\ 0 & 1/2 & 0 & 1/2\end{bmatrix}$.

The system matrix $A = K_1H^TK_2H = \begin{bmatrix}1/3 & 1/3 & 1/3 & 0\\ 1/6 & 5/12 & 1/6 & 1/4\\ 1/3 & 1/3 & 1/3 & 0\\ 0 & 1/2 & 0 & 1/2\end{bmatrix}$.

From the above example 1, the row sum of K_1H^T is 1 and similarily the row sum of K_2H is 1. It shows that A is a stochastic matrix in the sense that the row sum of A is 1 and each entry of A is non-negative.

2.2.2. Condition for Convergence

This section provides the condition for convergence. For further analysis, let me begin with the introduction of Perron-Frobenius theorem [4], which allows to find the condition for

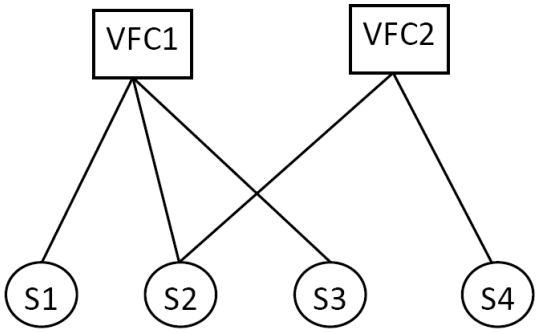

Figure 2.4. Tanner graph representation

convergence and also to determine the final consensus value.

Lemma 1- (Perron-Frobenius theory [4]): Let [A] be the transition matrix of an ergodic finite state Markov chain. Then $\lambda = 1$ is the largest real eigen value of [A], and $\lambda \geq |\lambda^{'|}$ for every other eigenvalue $|\lambda^{'|}$. Furthermore , $\lim_{m\to\infty}[A]^m = vw$, where w satisfying w[A]=w, and $v = (1, 1, ..., 1)^T$ is the unique right eigenvector of $\lambda = 1$, satisfying [A]v=v.

Proof - Let $[A]$ be a transition matrix of ergodic finite state Markov chain, for each non-zero column vector $x \geq 0$, L(x) is the largest real number L satisfying $Lx \leq [A]x$ where $\lambda = sup_{x\neq 0, x\geq 0} L(x)$. Then $L(x) = \min_{i;x_i>0} \frac{([A]x)_i}{x_i}$. For $x = (1, 1, ..., 1)^T$, $L(x) = \min_i \sum_j A_{ij} > 0$, so that $\lambda > 0$. If $\lambda^{'}$ be an arbitrary eigenvalue of $[A]$ (not necessarily real). Let x be a right eigenvector for $\lambda^{'}$. Taking the magnitudes of both sides of $\lambda^{'}x = [A]x$, for each component i

$$|\lambda^{'}||x_i| = |\sum_j A_{ij}x_j| \leq \sum_j A_{ij}|x_j|$$

Let $u = (|x_1|, |x_2|, ..., |x_j|)$, so the above equation becomes $|\lambda^{'}|u \leq [A]u$. Since $u \geq 0$, $u \neq 0$, it follows that $|\lambda^{'}| \leq L(u)$ and $L(u) \geq \lambda$, so $\lambda \geq |\lambda^{'}|$. Furthermore, if $|\lambda^{'}| = \lambda$, then $\lambda u \leq [A]u$, and from the properity of lemma 1 it follows that $\lambda u = [A]u$. Thus u is an eigenvector of $\lambda = |\lambda^{'}|$. Then $x = \beta u$ for some scalar β. It follows that x is an eigenvector of λ, so that $|\lambda^{'}| = \lambda$. Thus $\lambda > |\lambda^{'}|$ for all eigenvalues $|\lambda^{'}| \neq \lambda$.

This states that λ is the largest eigenvalue of all the other eigenvalues of $[A]$ and it is referred as dominant eigenvalue of $[A]$.

As $[A]$ be a stochastic irreducible matrix(i.e., the matrix of a markov chain consisting of a single recurrent class). Then $\lambda = 1$ is the largest real eigenvalue of $[A]$, $v = (1, 1, ..., 1)^T$ is the right eigenvector of $\lambda = 1$, unique within a scale factor, and there is a unique probability vector $w > 0$ that is a left eigenvector of $\lambda = 1$. Since each row of $[A]$ adds up to 1, $[A]v{=}v$. Any stochastic matrix, whether irreducible or not, has an eigenvalue $\lambda = 1$ with $v{=}(1, 1, ..., 1)^T$ as a right eigenvector.

Theorem 2: Consider a multi-group DSN represented by a tanner graph with routing matrix H. The consensus of the DSN is guaranteed if and only if there is at least a path between any pair of sensor nodes in the graph.

Proof- Now, consider the "if" direction. Since all the sensor nodes are connected, the system matrix A is irreducible. Moreover, the way A is generated informs that the underlining Markov chain for A is ergodic. Hence, from the Perron-Frobenius theorem [4], the following facts are known: 1) the dominant eigenvalue of A, λ_1, is 1 and strictly larger than the magnitudes of all other eigenvalues, and 2) the right eigenvector associated with it, v_1, is $1_{n\times 1}$. The two facts guarantee that the sensor nodes will reach the same value asymptotically.

To prove the "only if", note the fact that if sensor nodes are not connected, matrix A will have at least two eigenvalues at 1. The eigenvectors associated with all eigenvalues of "1" will contribute to the final consensus. Hence, the sensor nodes can not reach consensus.

Further analysis leads to two corollaries concerning the minimum number of communication links needed to establish a DSN that can reach consensus.

Corollary 2.1: Consider a multiple-group DSN that can reach consensus. The minimum number of communication links needed to form consensus is n.

Proof- For a DSN which has only one group and there is only one VFC that has communication with all n sensor nodes, the minimum number of communication links needed to form consensus is n.

Corollary 2.2: Consider a regular multiple-group DSN that can reach consensus. The minimum number of communication links needed to form consensus is $[\lfloor \frac{n}{m} \rfloor + 1]m$.

Proof- In order for a regular multiple-group DSN with m VFCs and n sensor nodes to reach consensus, the minimum number of sensor nodes in each group is $[\lfloor \frac{n}{m} \rfloor]$. Hence, the minimum number of communication links is $[\lfloor \frac{n}{m} \rfloor + 1]m$.

The two corollaries demonstrate the minimum number of communication links needed to establish consensus for two types of DSNs: a regular DSN and a general DSN. In order for the DSN to reach consensus and achieve consensus, the minimum number of links needed is greater than that of a general DSN. Although a single-group DSN has fewer communication links, this centralized configuration loses security, and more importantly, some communication links are difficult to establish due to the limitation on the range of communication linkage. In paper [3], it was shown through simulation that when the communication links in a regular DSN are subject to random switching (i.e., a communication link can randomly choose between pairs of VFCs and sensor nodes), the consensus may be reached faster. This simulation result can be conceptually explained as: when the communication topology changes from regular to irregular, the minimum number of links needed to establish consensus is reduced and the DSN has more flexibility in choosing paths to reach consensus. The random switching topology can speed up the consensus building process.

2.2.3. Final Consensus Value

Theorem 3: The final consensus value that the DSN converges to is $\frac{1}{1_{1\times m}H1_{n\times 1}} 1_{1\times m} Hx(0)$, where $x(0) \in R^{n\times 1}$ contains initial values of all sensor nodes in the DSN.

Proof- Decompose the system matrix A and rewrite equation 2.2.1 as

$$x[k] = \sum_{i=1}^{n} v_i \lambda_i^k w_i^T x[0], \tag{2.2.2}$$

Equation 2.2.2 informs that only the terms having eigenvalue 1 make contribution to the final values of sensor nodes.

In the case that the consensus condition is satisfied, the final value of $x[k]$ can be calculated as ${w_1}^T x[0]$. This means that the consensus value is a summation of each initial value scaled by the corresponding entry in the left eigenvector associated with the dominant eigenvalue 1. It can be easily checked that ${w_1}^T = \frac{1}{1_{1\times m} H 1_{n\times 1}} 1_{1\times m} H$, since it satisfies $w_1^T A = w_1^T$. The proof is complete.

Theorem 2 gives the condition for convergence of the consensus strategy and theorem 3 gives the dependence of consensus value on initial values of all sensor nodes. It is interesting to notice that the column sum of H matrix (as indicated by $1_{1\times m} H$) gives the weighting of each sensor node's contribution to the final consensus value. The column sum of H matrix is in fact the degree sequence of sensor nodes. Hence, the degrees of sensor nodes are the sole factors in determining the final consensus value. Interestingly, the degrees of VFCs do not impact the final consensus value. This observation naturally leads to the following corollary.

Corollary 2.3: Consider a multi-group DSN represented by a tanner graph with routing matrix H. Given that the DSN can reach consensus, the final consensus value is the average of all initial values if the degrees of all sensor nodes are the same.

Theorem 3 and corollary 2.3 specify the dependence of final consensus value on the column sum of H. This simple relationship allows to quickly design the routing matrix H to achieve certain consensus value. For instance, if certain sensors are known to measure data with high fidelity, or probe information with higher priority, it is reasonable to design the DSN in a way that such sensors have more contribution in the final consensus value. This inhomogeneous weighting can be achieved by assigning the important sensor nodes with higher degrees.

Now the theorem 3 is further illustrated with an example.

Example 2: Consider the DSN described by the tanner graph shown in figure 2.4. The routing matrix for this DSN is $H=\begin{bmatrix}1 & 1 & 1 & 0\\ 0 & 1 & 0 & 1\end{bmatrix}$.
The consensus can be reached as there exists at least a path between any two sensor nodes. Moreover, the consensus value is $\frac{1}{5}1_{1\times 2}\begin{bmatrix}1 & 1 & 1 & 0\\ 0 & 1 & 0 & 1\end{bmatrix}x(0) = \frac{1}{5}(x_1(0)+2x_2(0)+x_3(0)+x_4(0))$, where $x_1(0)$, $x_2(0)$, $x_3(0)$, and $x_4(0)$ represent the initial values of sensor nodes.

From example 1,

$K_1= [diag(\begin{bmatrix}1 & 2 & 1 & 1\end{bmatrix})]^{-1}= \begin{bmatrix}1 & 0 & 0 & 0\\ 0 & 1/2 & 0 & 0\\ 0 & 0 & 1 & 0\\ 0 & 0 & 0 & 1\end{bmatrix}$.

and $K_2= [diag(\begin{bmatrix}3 & 2\end{bmatrix})]^{-1}= \begin{bmatrix}1/3 & 0\\ 0 & 1/2\end{bmatrix}$.

The system matrix $A = K_1H^TK_2H = \begin{bmatrix}1/3 & 1/3 & 1/3 & 0\\ 1/6 & 5/12 & 1/6 & 1/4\\ 1/3 & 1/3 & 1/3 & 0\\ 0 & 1/2 & 0 & 1/2\end{bmatrix}$.
The final consensus value can be found by iteratively updating the dynamical equation $x[k+1] = Ax[k]$. When the number of iterations are large,

$lim_{k\to\infty}x(k) = lim_{k\to\infty}A^kx(0) = \begin{bmatrix}1/5 & 2/5 & 1/5 & 1/5\\ 1/5 & 2/5 & 1/5 & 1/5\\ 1/5 & 2/5 & 1/5 & 1/5\\ 1/5 & 2/5 & 1/5 & 1/5\end{bmatrix}x[0]$.

Hence, the consensus value is given by $x(\infty)= \left[\frac{1}{5}(x_1(0) + 2x_2(0) + x_3(0) + x_4(0))\right]$, which matches the result.

2.3. Dependence of Convergence Time on Network Structure

Convergence time is an important performance measure for consensus building strategies. In this section, the convergence time is related to the second largest eigenvalue of the system matrix A. The eigen-analysis provides an approach to directly infer convergence time from some very simple structural characteristics of a DSN, such as the number and degrees of sensor nodes and VFCs, etc.

From the last section, the dominant eigenvalue of system matrix A was proved to be $\lambda_1 = 1$ and its associated right eigen vector $v_1 = 1_{n\times 1}$. To find other eigenvalues of A, Courant Fischer theory along with the properities of spectral radius are used. The concept of spectral radius provides the dependence of convergence time on λ_2 whereas Courant Fischer theory concepts are used to relate λ_2 directly from its structure through routing matrix H.

2.3.1. Dependence of Convergence Time on λ_2

Theorem 4: Consider a DSN represented by a tanner graph with routing matrix H. Supposing that the DSN can reach consensus, the convergence time (i.e., the number of iterations such that the difference between sensor value and final consensus value is within δ of its initial value) is $log_{\lambda_2}\delta$ as $\delta \to 0$, where $\lambda_2 \neq 0$ is the second largest eigenvalue associated with the system matrix A.

Proof- From theorem 2, the values of sensor nodes converge to $x_f = v_1 w_1 x[0]$. There is only one eigenvalue with value 1, and all the other eigenvalues are real and have magnitude less than 1.

The case that $\lambda_2 = 0$ is trivial in that the consensus can be reached in one iteration. Lets focus on the case the $\lambda_2 \neq 0$.

$$x[k] = \sum_{i=1}^{n} v_i \lambda_i^k w_i^T x[0] = x_f + \sum_{i=2}^{n} v_i \lambda_i^k w_i^T x[0]. \quad (2.3.1)$$

Clearly, the spectral radius of $\sum_{i=2}^{n} v_i \lambda_i w_i^T$ is λ_2, which is equal to $\lim_{k\to\infty} ||(\sum_{i=2}^{n} v_i \lambda_i^k w_i^T)||^{\frac{1}{k}}$. In the limit of $\delta \to 0$, $k = log_{\lambda_2}\delta$ for $\frac{||x[k]-x_f||}{||x_0||} = \delta$.

From the above analysis, it implies that the convergence time is a function of the second largest eigenvalue λ_2 of the system matrix A, which is obtained from the routing matrix H. While this quantitative result is important and well known, it does not provide the convergence time from the DSN structure. In the next section, the structure of the routing matrix H to λ_2 is discussed, and in turn to the convergence time.

2.3.2. Dependence of λ_2 on Structure H

This section discusses on how to infer convergence time from its structure i.e, through the routing matrix H rather than the system matrix A. Initially let me discuss about Courant-fischer theorem to find eigenvalues of symmetric matrix and apply these concepts to this context.

Lemma 2-(Courant Fischer theory [17]): Courant Fischer theory provides an approach to calculate the eigenvalues of a symmetric matrix sequentially from the eigenvectors.
Let A be an $n \times n$ symmetric matrix with eigenvalues $\lambda_1 \geq \lambda_2 \geq ... \geq \lambda_n$ and corresponding eigenvectors $v_1, ..., v_n$. Then $\lambda_1 = \max_{||x||=1} x^T Ax$ and $\lambda_2 = max_{x\in S_1^{\perp}, ||x||=1} x^T Ax$. In general, for $1 \geq k \geq n$, let S_k denote the span of $v_1, ..., v_n$ (with S_0=0), and let $S_k^{\perp}$ denote the orthogonal complement of S_k. Then $\lambda_k = max_{x\in S_{k-1}^{\perp}, ||x||=1} x^T Ax$
Proof- Let A=$Q^T \lambda Q$ be the eigen decomposition of A. As $x^T Ax$=$x^T Q^T \lambda Qx$=$(xQ)^T \lambda (Qx)$, and since Q is orthogonal, $||Qx|| = ||x||$. Thus it suffices to consider the case when A is a diagonal matrix with the eigenvalues $\lambda_1, ..., \lambda_n$ in the diagonal. Then

$$x^T Ax = \begin{bmatrix} x_1 ..... x_n \end{bmatrix} \begin{bmatrix} \lambda_1 & & \\ & \ddots & \\ & & \lambda_n \end{bmatrix} \begin{bmatrix} x_1 \\ \vdots \\ x_n \end{bmatrix} = \sum_{i=1}^{n} \lambda_i x_i^2.$$

When A is diagonal, the eigenvectors of A are $v_k = e_k$, the standard basis vector in R^n, $i.e$,$(e_k)_i = 1$ if i=k, and $(e_k)_i = 0$ otherwise. Then the condition $x \in S_{k-1}^{\perp}$ implies $x \perp e_i$ for $i = 1, ..., k-1$, so $x_i = (x, e_i) = 0$. Therefore, for $x \in S_{k-1}^{\perp}$ with $||x|| = 1$, this shows

$$x^T A x = \sum_{i=1}^{n} \lambda_i x_i^2 = \sum_{i=k}^{n} \lambda_i x_i^2 \geq \lambda_k \sum_{i=k}^{n} x_i^2 = \lambda_k ||x||^2 = \lambda_k$$

On the other hand, plugging in $x = e_k \in S_{k-1}^{\perp}$ yields $x^T A x$=$(e_k)^T A e_k$=λ_k. This shows that

$$\lambda_k = max_{x \in S_{k-1}^{\perp}, ||x||=1} x^T A x \tag{2.3.2}$$

Similarly, for $||x|| = 1$,

$$x^T A x = \sum_{i=1}^{n} \lambda_i x_i^2 \leq \lambda_{max} \sum_{i=1}^{n} x_i^2 = \lambda_{max} ||x||^2 = \lambda_{max}$$

On the other hand, taking $x = e_1$, yields $x^T A x$=$(e_1)^T A e_1$=λ_{max}. Hence

$$\lambda_1 = \lambda_{max} = \max_{||x||=1} x^T A x$$

Theorem 5: The second largest eigenvalue of the system matrix A associated with a general DSN model represented by a tanner graph can be found as the maximum of $\sum_{i=1}^{m} (K_2^{\frac{1}{2}} H y)_i^2$, where $y \in R^{n \times 1}$ is subject to the following constraints: 1) $\sum_{i=1}^{n} y_i = 0$, 2) $\sum_{i=1}^{n} K_{1_i}^{-1} y_i^2 = 1$.

Proof- First, recall in the proof of theorem 1 that the eigenvalues of A are the same as the eigenvalues of the symmetric matrix $\hat{A} = K_1^{\frac{1}{2}} H^T K_2 H K_1^{\frac{1}{2}}$. Moreover, the left eigenvectors of $\hat{A}$ equals $w^T K_1^{1/2}$, where w^T is a left eigenvector of A.

Matrix $\hat{A}$ is symmetric. The Courant-Fischer theorem informs that the second largest eigenvalue λ_2 can be found as [17]

$$\begin{aligned} \lambda_2 &= max_{x \perp w_1^T K_1^{\frac{1}{2}}, ||x||=1} x^T \hat{A} x \\ &= max_{x \perp w_1^T K_1^{\frac{1}{2}}, ||x||=1} x^T K_1^{\frac{1}{2}} H^T K_2 H K_1^{\frac{1}{2}} x. \end{aligned}$$

Consider a new vector $y = K_1^{\frac{1}{2}}x$. Since w_1^T aligns with $1_{1\times n}K_1^{-1}$, y is subject to the constraint that $y \perp 1_{n\times 1}$. Moreover, since $||x|| = 1$, it implies $||K_1^{-\frac{1}{2}}y|| = 1$.

The second largest eigen value of the system matrix A associated with a general DSN model represented by a tanner graph can be found as the

$$\max \sum_{i=1}^{m} (K_2{}^{\frac{1}{2}} Hy)_i^2 \tag{2.3.3}$$

where $y \in R^{n\times 1}$ is subject to the following constraints: $1)\sum_{i=1}^{n} y_i = 0$, $2)\sum_{i=1}^{n} y_i^2 = 1$. Theorem 5 is very useful in that it allows the calculation of the second largest eigenvalue directly from the routing matrix H, rather than through the eigen-analysis of the system matrix A. The theorem provides an approach to obtain λ_2 from simple characteristics of the routing matrix H. In the following corollary, similar result for regular DSNs are provided.

Corollary 2.4: Considering a regular DSN, the second largest eigenvalue of the system matrix A can be found as the maximum of $\frac{1}{p}\sum_{i=1}^{m}(Hy)_i^2$, where p is the regular degree of VFCs, and where $y \in R^{n\times 1}$ is subject to the following constraints: 1) $\sum_{i=1}^{n} y_i = 0$, 2) $\sum_{i=1}^{n} K_{1_i}^{-1} y_i^2 = 1$.

Proof- This result can be derived directly from theorem 5, with the observation that K_2 equals $\frac{1}{p}I$.

Theorem 5 and corollary 2.4 provide an approach to obtain the second largest eigenvalue, and hence the convergence time for various subclasses of DSNs. Complementing the results in the consensus building literature [10, 11], the convergence time can be directly obtained from some simple structural characteristics for subclasses of DSNs. Theorem 6 considers a class of regular DSNs containing multiple groups, each of which has one leader that communicates to all other group leaders.

2.3.3. Finding Convergence Time for Various Structures

Theorem 6: Consider a regular DSN that contains m groups. Each group has 1 VFC and k sensor nodes that communicate with it. In each group, there is one and only one node that all VFCs communicate with (see figure 2.5). The consensus time for this regular DSN is $log_{\frac{k-1}{k+m-1}}\delta$.

Proof- The DSN considered in the theorem has m VFCs with regular degree $p = k+m-1$ and $n = mk$ sensor nodes. Without loss of generality, let me denote the sensor node with index $1 + k(i-1)$ as the one in group i that all VFCs communicate with. Moreover, for the convenience of presentation, let me introduce set S containing the indices of such sensor nodes for all groups, and set G_i containing the indices of all sensor nodes in group i.

In order to obtain λ_2, a slightly revised version of corollary 2.4 is used. Specifically, λ_2 is the maximum of $\frac{1}{p}\frac{\sum_{i=1}^{m}(Hy)_i^2}{\sum_{i=1}^{n}K_{1_i}^{-1}y_i^2}$, where y is subject to the constraint: $\sum_{i=1}^{n} y_i = 0$.

Now the relationship among y_i is obtained using Lagrange multipliers. Specifically, 1) all entries of y corresponding to the sensor nodes inside a group except the one that all VFCs communicate to are the same, i.e., y_j are equal for all $j \in G_i - S$ for each i from 1 to m. Now define the Lagrange operator L as

$$\begin{aligned} L &= \sum_{i=1}^{m}(Hy)_i^2 + \alpha(\sum_{i=1}^{n} y_i) + \beta(\sum_{i=1}^{n} K_{1_i}^{-1}y_i^2 - 1) \\ &= \sum_{i=1}^{m}(\sum_{j\in G_i+S} y_j)^2 + \alpha(\sum_{i=1}^{n} y_i) + \beta(\sum_{i=1}^{n} K_{1_i}^{-1}y_i^2 - 1) \end{aligned} \tag{2.3.4}$$

The optimal solution for (y_i, α, β) is the one that satisfies $\frac{\partial L}{\partial y_l} = 0$ for all l, $\frac{\partial L}{\partial \alpha} = 0$, and $\frac{\partial L}{\partial \beta} = 0$. $\frac{\partial L}{\partial y_l} = 0$ leads to

$$2\sum_{i=1,\&l\in G_i}^{m}(\sum_{j\in G_i+S} y_j) + \alpha + 2\beta K_{1_i}^{-1}y_l = 0 \tag{2.3.5}$$

Equation 2.3.5 informs that y_j are equal for all $j \in G_i - S$ for each i from 1 to m.

Finally, the maximum of $\frac{\sum_{i=1}^{m}(Hy)_i^2}{\sum_{i=1}^{n}K_{1_i}^{-1}y_i^2}$ is obtained using the constraint that $\sum_{i=1}^{n} y_i = 0$,

$$\frac{\sum_{i=1}^{m}(Hy)_i^2}{\sum_{i=1}^{n}K_{1_i}^{-1}y_i^2} = \frac{\sum_{i=1}^{m}(\sum_{j\in G_i+S}y_j)^2}{\sum_{i\notin S}y_i^2 + m\sum_{i\in S}y_i^2} = \frac{\sum_{i=1}^{m}(\sum_{j\notin G_i+S}y_j)^2}{\sum_{i\notin S}y_i^2 + m\sum_{i\in S}y_i^2} \tag{2.3.6}$$

since $\sum_{j\in G_i+S}y_j = -\sum_{j\notin G_i+S}y_j$. The upper bound of the right side of equation 2.3.6 can be found as

$$\frac{\sum_{i=1}^{m}(\sum_{j\notin G_i+S}y_j)^2}{\sum_{i\notin S}y_i^2 + m\sum_{i\in S}y_i^2} \leq \frac{\sum_{i=1}^{m}(\sum_{j\notin G_i+S}y_j)^2}{\sum_{i\notin S}y_i^2}, \tag{2.3.7}$$

since y_i^2 for $i \in S$ does not appear in the denumerator and is greater than 0. The equality holds when $y_i = 0$ for all $i \in S$.

Applying the constraints that $\sum_{i=1}^{n}y_i = 0$, $y_i = 0$ for $i \in S$, and y_j are equal for all $j \in G_i - S$ for each i from 1 to m, the right side of equation 2.3.7 is simplified as

$$\frac{\sum_{i=1}^{m}(\sum_{j\notin G_i+S}y_j)^2}{\sum_{i\notin S}y_i^2} = \frac{\sum_{i=1}^{m}(\sum_{j\in G_i-S}y_j)^2}{\sum_{i\notin S}y_i^2} = (k-1)\frac{\sum_{i\notin S}y_i^2}{\sum_{i\notin S}y_i^2} = k-1$$

Hence, the maximum of $\frac{\sum_{i=1}^{m}(Hy)_i^2}{\sum_{i=1}^{n}K_{1_i}^{-1}y_i^2} = k-1$. Since the second largest eigenvalue λ_2 is the maximum of $\frac{1}{p}\frac{\sum_{i=1}^{m}(Hy)_i^2}{\sum_{i=1}^{n}K_{1_i}^{-1}y_i^2}$, it implies $\lambda_2 = \frac{k-1}{k+m-1}$.

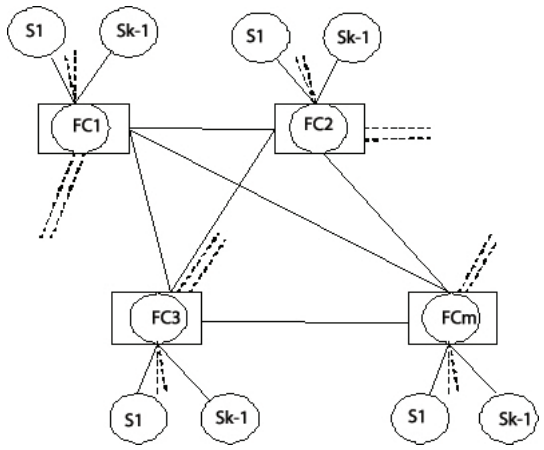

Figure 2.5. DSN structure.

Theorem 6 says that for a common class of DSN that contains multiple groups, in each of which exists a leader that communicates to all the other leaders, the consensus time using

the iterative averaging algorithm is only dependent on the number of groups, together with the number of nodes in each group. The results on the explicit relationship of DSN structure and the consensus time is very valuable due to the scalability and facilitation of design. Here, in the following example the theorem is illustrated concerning a DSN with only three groups. However, it is important to note that the value of the theorem resides in large-scale networks, for which the consensus time can be inferred directly from simple characteristics of DSN structures, without any complicated computation.

Example 3: A DSN consisting of three groups is shown in figure 2.6a. Each group has one fusion center (leader) and three sensor nodes communicating with the fusion center. Each group leader communicates to the other two group leaders. The tanner graph representation is shown in figure 2.3b with $k = 4$ and $m = 3$. According to theorem 6, the second largest eigenvalue is 0.5, and the consensus time is $log_{0.5}\delta$.

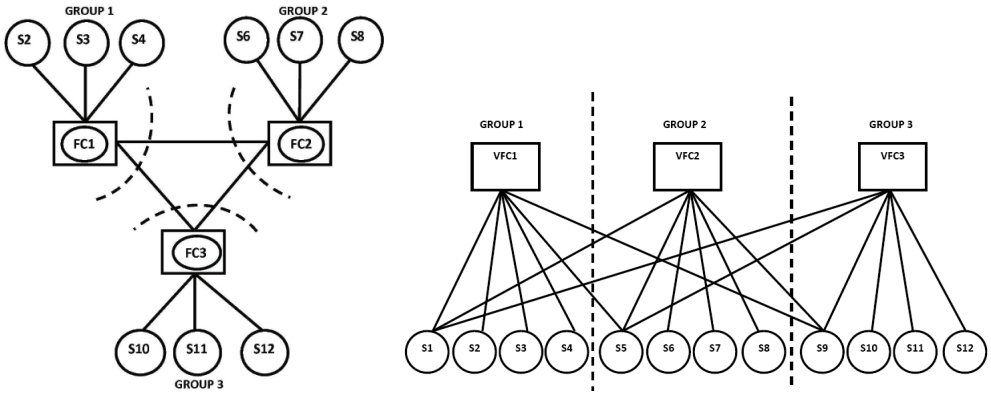

Figure 2.6. a) The DSN with fusion centers considered in example 3; b) The tanner graph representation

The next theorem considers another class of DSN which is regular and containing two VFCs. The consensus time can be directly inferred from the regular degree and the number of sensor nodes in the DSN. The theorem is exemplified in example 4.

Theorem 7: Consider a DSN containing two VFCs with regular degree p and n sensor nodes. Supposing that the DSN can reach consensus, the consensus time is $log_{\frac{n-p}{p}}\delta$.

Proof- For the analysis, introduce set S containing the sensor nodes that communicate with both VFCs, and set G_i containing the sensor nodes only communicating with VFC i. Similar to the proof of theorem 6, it implies that y_j are the same for $j \in G_i$, for each i.

Now lets calculate λ_2 as the the maximum of $\frac{1}{p}\frac{\sum_{i=1}^{m}(Hy)_i^2}{\sum_{i=1}^{n}K_{1_i}^{-1}y_i^2}$. Using the constraint that $\sum_{i=1}^{n} y_i = 0$, and the condition that y_j are the same for $j \in G_i$, for each i, it shows that

$$\begin{aligned}
\frac{1}{p}\frac{\sum_{i=1}^{m}(Hy)_i^2}{\sum_{i=1}^{n}K_{1_i}^{-1}y_i^2} &= \frac{1}{p}\frac{(\sum_{i\in S+G_1} y_i)^2 + (\sum_{i\in S+G_2} y_i)^2}{\sum_{i\in G_1} y_i^2 + \sum_{i\in G_2} y_i^2 + 2\sum_{i\in S} y_i^2} \\
&= \frac{1}{p}\frac{(\sum_{i\in G_2} y_i)^2 + (\sum_{i\in G_1} y_i)^2}{\sum_{i\in G_1} y_i^2 + \sum_{i\in G_2} y_i^2 + 2\sum_{i\in S} y_i^2} \\
&\leq \frac{1}{p}\frac{(\sum_{i\in G_2} y_i)^2 + (\sum_{i\in G_1} y_i)^2}{\sum_{i\in G_1} y_i^2 + \sum_{i\in G_2} y_i^2} \\
&= \frac{1}{p}\frac{(n-p)(\sum_{i\in G_1} y_i^2 + \sum_{i\in G_2} y_i^2)}{\sum_{i\in G_1} y_i^2 + \sum_{i\in G_2} y_i^2} = \frac{n-p}{p}
\end{aligned}$$

The equality holds when $y_i = 0$ for all $i \in S$. The proof is complete.

Example 4: Consider a regular DSN that has two VFCs with regular degree 6 and 8 sensor nodes (shown in figure 2.7). According to theorem 7, the second largest eigenvalue is $\frac{2}{5}$, and the consensus time is therefore $log_{0.4}\delta$.

The next theorem considers an irregular DSN that has one and only one sensor node that communicates with all VFCs.

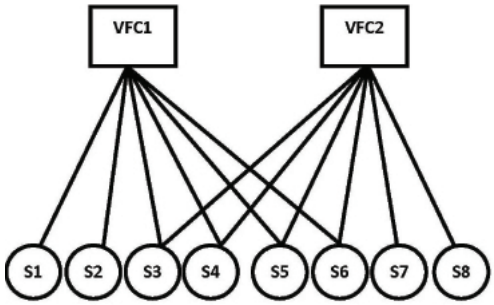

Figure 2.7. The tanner graph representation for the DSN in example 3.

Theorem 8: Consider a DSN that contains $m \geq 3$ groups (see figure 2.8). Each group has 1 VFC and k sensor nodes that communicate with it. There exists one and only one sensor node in the DSN that communicates with all VFCs. The consensus time for this DSN is $log_{\frac{k}{k+1}} \delta$.

Proof-The DSN considered in the theorem has m VFCs and $n = mk$ sensor nodes. Consider G_i to indicate the set, containing the indices of sensor nodes in group i. Without loss of generality, assume that the index of the sensor node communicating with all VFCs is 1, and the group containing this particular sensor node is group 1. Moreover, assume that the sensor nodes in group i are indexed from $k(i-1)+1$ to ki.

Now use the theorem 5 to obtain λ_2, which is the maximum of $\frac{\sum_{i=1}^{m}(K_2^{\frac{1}{2}}Hy)_i^2}{\sum_{i=1}^{n} K_{1_i}^{-1} y_i^2}$, where y is subject to the constraint: $\sum_{i=1}^{n} y_i = 0$. Using Lagrange multipliers, it shows that all entries of y corresponding to the sensor node inside a group $G_i - \{1\}$ for each i from 1 to m are the same. This result is discussed in the proof of theorem 6. Using these constraints, the following equation reduces to

$$\begin{aligned} \frac{\sum_{i=1}^{m}(K_2^{\frac{1}{2}}Hy)_i^2}{\sum_{i=1}^{n} K_{1_i}^{-1} y_i^2} &= \frac{\sum_{i=1}^{m}(K_2^{\frac{1}{2}}\sum_{j\in G_i+\{1\}} y_j)^2}{\sum_{i\notin\{1\}} y_i^2 + m\sum_{i\in\{1\}} y_i^2} \\ &= \frac{\sum_{i=1}^{m}(K_2^{\frac{1}{2}}\sum_{j\notin G_i+\{1\}} y_j)^2}{\sum_{i\in G_1-\{1\}} y_i^2 + \sum_{i\notin G_1} y_i^2 + m\sum_{i\in\{1\}} y_i^2} \end{aligned} \tag{2.3.8}$$

$$
\begin{aligned}
&\leq \frac{\sum_{i=1}^{m}(K_2^{\frac{1}{2}}\sum_{j\notin G_i+\{1\}} y_j)^2}{\sum_{i\in G_1-\{1\}} y_i^2+\sum_{i\notin G_1} y_i^2} \\
&= \frac{(K_2^{\frac{1}{2}}\sum_{j\in G_1-\{1\}} y_j)^2+\sum_{i=2}^{m}(K_2^{\frac{1}{2}}\sum_{j\in G_i} y_j)^2}{\sum_{i\in G_1-\{1\}} y_i^2+\sum_{i\notin G_1} y_i^2} \\
&= \frac{(\frac{1}{k})(\sum_{i\in G_1-\{1\}} y_i)^2+(\frac{1}{k+1})(\sum_{i=2}^{m}(\sum_{j\in G_i} y_j)^2)}{\sum_{i\in G_1-\{1\}} y_i^2+\sum_{i\notin G_1} y_i^2} \\
&= \frac{(\frac{(k-1)^2}{k})y_2^2+(\frac{k^2}{k+1})\sum_{i=2}^{m} y_{k(i-1)+1}^2}{(k-1)y_2^2+\sum_{i=2}^{m} k y_{k(i-1)+1}^2}
\end{aligned}
$$

Denoting y_2^2 be X and $\sum_{i=2}^{m} y_{k(i-1)+1}^2$ be Y, the above equation becomes

$$
\begin{aligned}
\frac{\frac{(k-1)^2}{k}X+\frac{k^2}{(k+1)}Y}{(k-1)X+kY} &= \frac{(k-1)[\frac{1}{k}((k-1)X+kY)+\frac{k^2}{(k+1)(k-1)}Y-Y]}{(k-1)X+kY} \\
&= \frac{k-1}{k}+\frac{\frac{k^2}{k+1}Y-(k-1)Y}{(k-1)X+kY} \\
&\leq \frac{k-1}{k}+\frac{\frac{k^2}{k+1}Y-(k-1)Y}{kY} \\
&= \frac{k}{k+1}
\end{aligned}
$$

The equality holds when $y_{i\in G_1}=0$.

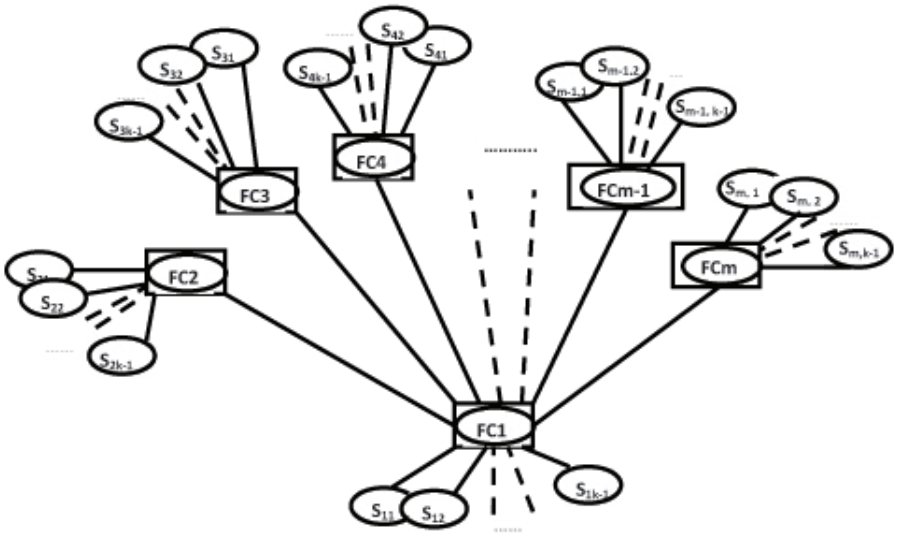

Figure 2.8. The DSN structure considered in theorem 8.

Example 5: Consider a irregular DSN that has 3 groups . Each group has 1 VFC and 3 sensor nodes that communicate with it. Only one sensor node in the structure communicates with all the other VFCs (figure 2.9), then the second largest eigenvalue is $\frac{3}{4}$, and the consensus time is therefore $log_{0.75}\delta$.

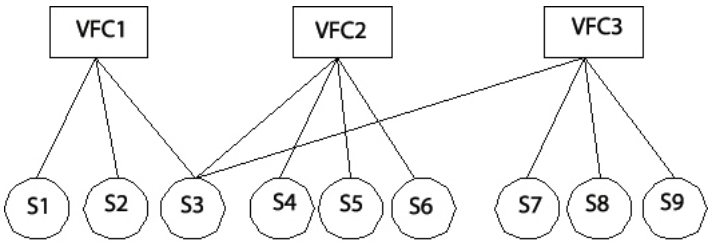

Figure 2.9. The tanner graph representation for the DSN in example 5.

Theorems 6, 7, and 8 demonstrate three classes of DSNs, whose consensus time can be directly obtained from connectivity structures using theorem 5. Using this approach, similar results for other classes of DSNs can be obtained, including irregular DSNs. By linking eigenvalues with the properties of the routing matrix rather than the system matrix A directly, rich structural information is exposed to aid in the network design and analysis. The inference of eigenvalue from the structure of graphs (especially asymmetric graphs) is not a trivial task. This work provides an interesting approach to expose hidden graph structure that is not obvious from the graph directly associated with network dynamics; such hidden structure may help to address algebraic graph problems with rich insight.

These results also provide a direct approach to DSN design. First, the degrees for sensor nodes can be selected to reach desired consensus value. Consensus time can also be achieved through the DSN design. For instance, for the class of DSNs considered in theorem 6, the number of VFCs for any convergence time predefined can be chosen, by using the explicit relation between λ_2 and the number of VFCs. Consider a network containing 1000 sensor nodes and the desired convergence time of 10 (associated with $\delta = 0.01$). According to the structure

related to theorem 6, m is found to be 25 by solving for $log_{\frac{\frac{1000}{m}-1}{\frac{1000}{m}+m-1}} 0.01 \leq 10(\log_{\lambda_2} \delta \leq k)$. The results are particularly useful when large-scale networks are considered for which existing solutions for computing convergence times such as the numerical semi-definite programming (SDP) can be very time-consuming [9]. Similarly, for the class of DSNs considered in theorem 7, the regular degree of VFCs are chosen for any desired convergence time. The approach to consensus analysis and design in this paper can be extended to other iterative consensus algorithms, and DSNs described by graphs other than tanner graphs, e.g., hierarchical graphs.

2.4. Analysis for Other Graphical Models

The results presented so far are focused on bipartite graphical models. However, they can easily be extended to other graphical models as well. For instance, consider a hierarchical tree structure that is commonly used to represent a DSN. The system dynamics for a 2-layer hierarchical structure can easily be captured by $x[k+1] = K_1 H_1^T (K_3 H_2^T K_4 H_2) K_2 H_1 x[k]$, where H_1 and H_2 are the routing matrices associated with the first and second layers respectively, and $K_1 = [diag(H_1^T 1)]^{-1}$, $K_2 = [diag(H_1 1)]^{-1}$, $K_3 = [diag(H_2^T 1)]^{-1}$, and $K_4 = [diag(H_2 1)]^{-1}$. For instance, the dynamics of the hierarchical network shown in figure 2.1b can be represented by

$$x[k+1] = \begin{bmatrix} 1_{1\times 4} & & \\ & 1_{1\times 4} & \\ & & 1_{1\times 4} \end{bmatrix}^T \left(\begin{bmatrix} 1 & 1 & 1 \end{bmatrix}^T \begin{bmatrix} \frac{1}{3} & \frac{1}{3} & \frac{1}{3} \end{bmatrix} \right) \begin{bmatrix} 0.25_{1\times 4} & & \\ & 0.25_{1\times 4} & \\ & & 0.25_{1\times 4} \end{bmatrix} x[k].$$

Explicit results characterizing the convergence behavior, similar to those derived for the bipartite graphical models, can also be derived for hierarchical graphical models.

CHAPTER 3

LONG TERM INVESTMENT IN THE NATIONAL AIRSPACE SYSTEM

3.1. Background and Problem Description for Long Term Investment in the National Airspace System

3.1.1. Introduction

The demand for air travel has increased considerably over the years and is still increasing. Because of the rapid increase in demand, the number of aircraft operations (i.e., arrival and departure) in the airport is also increasing. The major role of controllers at airports is to handle all those operations to ensure proper safety and reduce delays. But the limited capacity of constrained resources like runways, navigation tools, etc cause big problems for managing the aircraft operations in enroute and in terminal areas.

In a survey of transportation statistics [26], one in four arriving flights was delayed by more than 15 minutes at major airports in the United States. These delays increase the operating cost of aircraft, and in turn impact the passengers in terms of higher airfare and delayed service time [35]. The delays have negative effects on the demand, which reduces the future growth non-linearly. This affects the entire national airspace over the following years by decreasing the revenues to the nation as well as the connectivity of markets among the nations. Hence, it is necessary to react quickly to the problem of congestion and find a solution. Investment in increasing the capacity of airports becomes the main way to reduce delays, and also should ensure that minimum capacity delivery costs(investment to increse the capacity resources) are maintained.

Although various studies are concerned with the investment problem [30, 35], very little work has considered a systematic planning design that minimizes the total delays in the NAS

in the long run. In this thesis, the congestion problem is modeled by considering the entire national airspace as a network with aircraft transitting among airports modeled as flows among nodes/agents. The total delays in the network are optimized over a period of time with respect to contraints such as capacity delivery costs. This modeling approach is aimed to answer the key issues in planning such as where, when, and how much to increase the capacity.

3.1.2. Conceptual Problem Description

Traffic delays can be minimized by allocating new capacity resources at congested airports. Paper [35] discussed the problem of congestion reduction by providing an optimal capacity increase strategy over a period of time after the congestion threshold is reached. The optimal case is chosen to yield more profits to the investors. But the problem is only concerned with a single congested airport. Here, a network of airports are considered instead of a single congested airport so that the entire NAS performance is used for the design of optimal planning strategies.

The motivation for this approach is that the performance is not affected solely by an individual airport because aircraft travel from one airport node to another node. Considering the growing demand, the flow among airport nodes is modeled using a network model to maximize the capacity performance over the national airspace system. The network model abstracts the key issues like where, when and how much to increase the capacity. A mathematical optimization problem over a period of time is formulated, and the solution to the optimization problem should help to answer these key issues.

Here, the focus is on long term investment with consideration of the growth in demand. Similar to the long term approach, [30] focused on increasing capacity constrained resources by 2015 and 2025 but their approach is limited to building new runways. In the later sections, the relevant literature work related to the proposed problem is discussed, and in section 3.2 the basics of queueing models and their analysis are provided. In section 3.3, a preliminary

network model is presented, and finally in section 3.4, a mathematical optimization problem is formulated to solve the investment problem.

3.1.3. Literature Review

Research evaluating the needs for capacity-constrained airports has been addressed in various studies. In a closely related work [35], the congestion problem is addressed by considering a single airport. Congestion threshold, amount of capacity increase and years to increase capacity are the key design parameters. The proposed model provides various strategies, and the difference between the considered strategies with the usual scenario is calculated. The design of strategies has the benefit of reacting quickly to changes of demand. The limitation of this model is that it models an individual congested airport instead of considering the whole network.

Long term future airport capacity tasks (FACT) was considered in [30] to assess the capacity-constrained airports with the goal of identifying airports that need additional capacity over different time frames (2007, 2015, 2025). The analysis considered airports and metropolitan areas over the NAS in the United States, and the planned improvements where taken into account while modeling. They are new runway constructions, airspace redesign, new or revised air traffic control procedures and new Nextgen technological improvements.
FACT description [30]- The model forecasts the demand and capacity, and specific thresholds are used to locate the capacity-constrained airports according to four assessments. The demand is forecasted using terminal area forecast (TAF) which predicts demand on airport by airport, and future air traffic estimator (FATE) predicts traffic between origin to destination metropolitan areas, and then restated on airport by airport basis. The capacity is forecasted using annual service volume (ASV) which estimates the average delay assocaited with the level of aircraft operations, and NAS modeling considers benchmark capacity which measures the average delay associated with the demand. The capacity-contrained airports are those

that satisfy all four forecasted assessments. The assessments include ratio of TAF to ASV and FATE to ASV exceeding threshold level of 0.8, arrival queuing delay exceeding 12 minutes, and the delays caused by local conditions being more than 50 percent while calculating NAS with TAF and FATE demand forecasts.

Limitations of the model [30]- The limitations of the model are that the forecasted demand assumptions are considered prior to economic downturn, and analytical reasoning of specific threshold values are not included. It considers runways as the sole capacity constraints and concludes with building new runways to increase the capacity to reduce the delays. Whereas in this thesis, a mathematical model is provided which abstracts the key issues like how much to increase the capacity, based on the time period and the allocated money.

Few authors [29, 31] have considered network models for NAS but their models have not been extended to identify the capacity needs for the long-term. A network model is considered in [31] for air traffic over the NAS. This model is quite similar to our model in the sense that it considers flow restrictions only at the boundaries of airport nodes rather than the enroute areas. A network model for air traffic in the NAS was considered in [29] to analyze the impact of trajectory uncertainity and precision on air traffic flow by converting uncertainities to queueing parameters and establishing relation between parameters and air traffic flow efficiency. The netwok model for abstracting restrictions and developing strategies to reduce congestion over the NAS was considered in [34]. My work focuses on modeling air traffic over NAS as a network model and maximizing the performance in the network over a long term.

3.2. Queueing Models

In the NAS, the flow of aircraft is affected by uncertainities like take-off times, unpredicitable weather conditions, and other factors. These make the controllers difficult to predict the position of the aircraft in advance. Thus, it becomes extremely difficult to schedule the

operations of the flow (we refer group of aircrafts as flow). Hence, the behavior of flow is modeled as stochastic and the flow is restricted using a queueing representation to ensure proper arrivals and departures in the downstream region. Consider an example of a simple queue; if a controller at Dallas airport is expecting a flight from Houston to Dallas, due to an uncertain take-off time, the flight from Memphis to Dallas arrived at the same time. The controller at Dallas airport cannot allocate the same runway to both the flights. Hence the flights are queued and served based on first input, first output (FIFO). If the flight from Memphis to Dallas approaches the queue intially, the flight from Houston to Dallas is queued and served based on its service time.

Queueing models are used to capture the impact of management on flows [36]. It is essentially used in various research to model air traffic flow over the NAS. M/G/1 queueing model was considered in [35], and M/M/n and M/D/1 queuing models were considered in [32]. In the next section, the nature of arrivals and service present in queueing theory are discussed.

3.2.1. Poisson Arrivals and Various Service Models

This section is based on the reference of fundamentals of Queuing theory [36]. As discussed earlier about the stochastic nature of flow, here the number of arrivals in a time interval and the probability distribution of time describing successive arrivals i.e, interarrival times are discussed.

Consider the arrival process where $N(t)$ denotes number of arrivals up-to time t, with N(0)=0, and which satisfies the following three assumptions:

1) The probability occurance of an arrival between time t and $t + \delta t = \lambda \delta t + o(\delta t)$, where λ is the flow rate independent of $N(t)$, δt is the increment in time and $o(\delta t)$ denotes a quantity that is negligible when compared to δt as $\delta t \to 0$

$$\lim_{\delta t \to 0} \frac{o(\delta t)}{\delta t} = 0$$

2) The probability occurance of more than one arrival between t and $t+\delta t$=$o(\delta t)$.

3) The numbers of arrival in non-overlapping intervals are statistically independent.

Now calculate the probability occurance of n arrivals in time interval of t, n being an integer ≥ 0.

Considering the case $n \geq 1$,

$p_n(t+\delta t)$= Pr(n arrivals in t and none in δt)+ Pr($n-1$ arrivals in t and one in δt)+....+ Pr(no arrivals in t and n in δt)

Incorporating the three assumptions to the above equation, it reduces to

$$p_n(t+\delta t) = p_n(t)[1-\lambda\delta t - o(\delta t)] + p_{n-1}(t)[\lambda\delta t + o(\delta t)] + o(\delta t) \tag{3.2.1}$$

where the last term, $o(\delta t)$ represents the term Pr($n-j$ arrivals in t and j in δt): $2 \leq j \leq n$.

Rewriting equation 3.2.1,

$$[p_n(t+\delta t) - p_n(t) = -\lambda\delta t p_n(t) + \lambda\delta t p_{n-1}(t) + o(\delta t)] \rightarrow (n \geq 1)$$

$$\mathrm{p}_0(t+\delta t) - p_0(t) = -\lambda\delta t p_0(t) + o(\delta t) \rightarrow (n = 0)$$

Dividing the above equations by δt with $\delta t \rightarrow 0$,

$$\frac{dp_n(t)}{dt} = -\lambda p_n(t) + \lambda p_{n-1}(t) \rightarrow (n \geq 1)$$

$$\frac{dp_0(t)}{dt} = -\lambda p_0(t) \rightarrow (n = 0)$$

for case $n = 0$, $p_0(t) = e^{-\lambda t}$, and for case $n = 1$, it shows that

$$p_1(t) = \lambda t e^{-\lambda t} \tag{3.2.2}$$

Generalising equation 3.2.2, probability occurance of n arrivals in time interval of t can be found as

$$p_n(t) = \frac{(\lambda t)^n}{n} e^{-\lambda t} \tag{3.2.3}$$

Equation 3.2.3, tells that the probability distribution of the number of arrivals in a time interval t follows a poisson distribution.

Now consider the probability distribution of interarrival times. Let T be a random variable describing the time between successive time arrivals, then

Pr($T \leq t$)=1-$p_0(t) = 1-e^{\lambda t}$.

Thus T follows an exponential distribution with mean $\frac{1}{\lambda}$. This implies that the probability distribution describing the time of successive arrivals follows exponential distribution.

Distribution of service time- The distribution of service time can follow either a general distribution, exponential distribution, or deterministic. In this model, the concepts of general distribution of service time are applied to formulate the mathematical equation for delays in the network.

Queueing system modeling depends on the number of servers. The servers can be 1 to infinity. In this model a single server system is considered. The server restricts the flow according to the service time.

3.2.2. Performance Analysis

This section is based on the reference of fundamentals of queuing theory [36]. Backlog is the number of aircraft restricted within a boundary region so as to allow smooth downstream flow and ensure less congestion in the downstream region. Backlog is a parameter directly proportional to delay. Here the calculation of the backlog for poisson arrivals and the general distribution of service time are discussed. Minimizing backlogs/delays in the NAS is the goal for our long-term planning problem to maximize the performance.

Backlog in terms of general distribution service time [36]- Consider the case of a single server queue with poisson arrivals and general distribution service time. Let λ be the arrival

rate and S be the random variable describing the general distribution service time. Let $\mu = \frac{1}{E[S]}$ be the service rate . Assume $\frac{\lambda}{\mu} < 1$.

Consider a flight arriving to the queue. Its delay is determined by the number of flights already in queue waiting for being served, and by the number of flights already in service. If it is a single server queue then the number of flights already in service is 1. Now consider there are L_q number of flights already in the queue, each contributing an average delay of $E[S]$. Thus the average delay caused due to the flights in queue is $L_q E[S]$. Now consider the delay contributed by the flight already in service. It has completed some of its service already, so its contribution to the delay is its remaining service time, but not the total service time. Its remaining service time is determined as Pr(server busy)$\times$ E[residual service time|server busy] Thus the average delay for the arriving flight is

$$W_q = L_q E[S] + \text{Pr(server busy)} \times \text{E[residual service time|server busy]}$$

As $L_q = \lambda W_q$, the above equation reduces to

$$W_q = \frac{Pr(server\ busy).E[residual\ service\ time|server\ busy]}{1-\lambda E[S]}$$

Since the Pr(server busy) as the probability that arriving flight finds server busy is $\lambda E[S]$, the expected residual service time conditional on the arrival flight finding server busy is

$$\text{E[residual service time|server busy]} = \frac{E[S^2]}{2E[S]} = \frac{E^2[S]+var[S]}{2E[S]} = \frac{1+\frac{var[S]}{E^2[S]}}{2} E[S]$$

Thus, the total delay for the arriving flight is given by

$$W_q = \frac{1+\frac{var[S]}{E^2[S]}}{2} \frac{\lambda E[S]}{1-\lambda E[S]} E[S]$$

As the length of the queue for arriving flight (Backlog) is $B_q = W_q \lambda$

Therefore B_q can be written as

$$B_q = \frac{1 + \frac{var[S]}{E^2[S]}}{2} \frac{\lambda^2 E[S]}{1 - \lambda E[S]} E[S] \tag{3.2.4}$$

Backlog in terms of exponential distribution service time For a exponential distribution, var[S]=E^2, then equation 3.2.4 reduces to

$$B_q = \frac{\lambda^2 E[S]}{1-\lambda E[S]} E[S]$$

Backlog in terms of deterministic service time For a determnistic service with time T, var[S]=0, then equation 3.2.4 reduces to

$$B_q = \frac{\lambda^2 T^2}{2(1-\lambda T)}$$

3.3. A Preliminary Network Model for the NAS

A network model contains a number of airport nodes where there is a flow from one node to another. It considers the flow interactions over the entire NAS. Now consider the flow rate at airport node j as λ_j. It is the summation of flows originating at other nodes and terminating at node j, which is represented by the following equation

$$\lambda_j = \sum_{i=1}^{n} \lambda_{ij} \tag{3.3.1}$$

An example of network containing 3 origin airports shown in figure 3.1, where $\lambda_j = \sum_{i=1}^{3} \lambda_{ij} = \lambda_{1j} + \lambda_{2j} + \lambda_{3j}$.

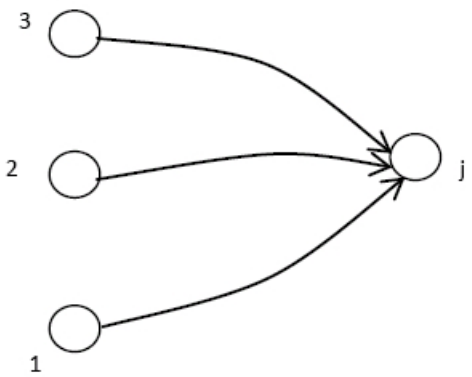

Figure 3.1. Flow rate at node j

In a network of n nodes, the airport node i contributes weighted average w_{ij} of its total flow to node j, whereas remaining weighted average $1 - w_{ij}$ is contributed to other nodes in

the network except j. Lets define a matrix W which captures the merging/splitting of flows in the NAS. W is called as weighted average matrix.

$$W_{n\times n} = \begin{bmatrix} w_{11} & w_{12} & w_{13} & .... & w_{1n} \\ w_{21} & w_{22} & w_{23} & .... & w_{2n} \\ . & . & . & .... & . \\ . & . & . & .... & . \\ w_{n1} & w_{n2} & w_{n3} & .... & w_{nn} \end{bmatrix}$$

For $i = j$ there is no flow, w_{11}, w_{22},....,w_{nn}=0, therefore

$$W_{n\times n} = \begin{bmatrix} 0 & w_{12} & w_{13} & .... & w_{1n} \\ w_{21} & 0 & w_{23} & .... & w_{2n} \\ . & . & . & .... & . \\ . & . & . & .... & . \\ w_{n1} & w_{n2} & w_{n3} & .... & 0 \end{bmatrix}$$

Therefore equation 3.3.1 can be written in terms of matrix W as

$$\lambda_j = \sum_{i=1}^{n} \lambda_{ij} = \sum_{i=1}^{n} \lambda_i w_{ij} \tag{3.3.2}$$

Here the whole network structure is illustrated through a simple network containing 4 airport nodes namely Seattle, San Francisco (SF), Los Angeles (LA), and Denver. There exists flow interactions among these nodes (see figure 3.2). Let W captures the weighted averages of the flow in the network.

Let

$$W_{4\times 4} = \begin{bmatrix} w_{Seattle-Seattle} & w_{Seattle-SF} & w_{Seattle-LA} & w_{Seattle-Denver} \\ w_{SF-Seattle} & w_{SF-SF} & w_{SF-LA} & w_{SF-Denver} \\ w_{LA-Seattle} & w_{LA-SF} & w_{LA-LA} & w_{LA-Denver} \\ w_{Denver-Seattle} & w_{Denver-SF} & w_{Denver-LA} & w_{Denver-Denver} \end{bmatrix}$$

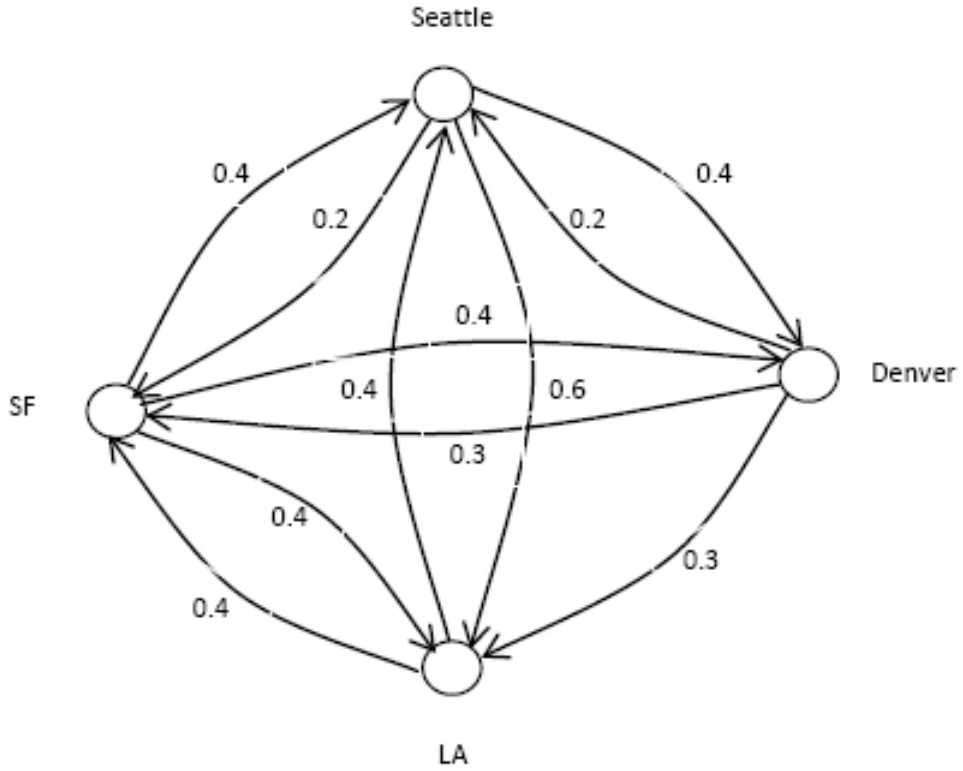

Figure 3.2. Flow representation with weighted averages from each airport node

$$W_{4\times4} = \begin{bmatrix} 0 & 0.4 & 0.4 & 0.2 \\ 0.2 & 0 & 0.4 & 0.4 \\ 0.4 & 0.6 & 0 & 0 \\ 0.4 & 0.3 & 0.3 & 0 \end{bmatrix} \tag{3.3.3}$$

Using equation 3.3.2 the flow rate at each node is

$$\begin{aligned} \lambda_{Seattle} &= \sum_{i=1}^{4} \lambda_{iSeattle} = \sum_{i=1}^{4} \lambda_i w_{iSeattle} \\ &= \lambda_{Seattle} w_{Seattle-Seattle} + \lambda_{SF} w_{SF-Seattle} + \lambda_{LA} w_{LA-Seattle} + \lambda_{Denver} w_{Denver-Seattle} \\ &= \lambda_{Seattle} 0 + \lambda_{SF} 0.4 + \lambda_{LA} 0.4 + \lambda_{Denver} 0.2 \\ &= \lambda_{SF} 0.4 + \lambda_{LA} 0.4 + \lambda_{Denver} 0.2 \end{aligned}$$

$$\begin{aligned}
\lambda_{SF} &= \sum_{i=1}^{4} \lambda_{iSF} = \sum_{i=1}^{4} \lambda_i w_{iSF} \\
&= \lambda_{Seattle} w_{Seattle-SF} + \lambda_{SF} w_{SF-SF} + \lambda_{LA} w_{LA-SF} + \lambda_{Denver} w_{Denver-SF} \\
&= \lambda_{Seattle} 0.2 + \lambda_{SF} 0 + \lambda_{LA} 0.4 + \lambda_{Denver} 0.4 \\
&= \lambda_{Seattle} 0.2 + \lambda_{LA} 0.4 + \lambda_{Denver} 0.4
\end{aligned}$$

$$\begin{aligned}
\lambda_{LA} &= \sum_{i=1}^{4} \lambda_{iLA} = \sum_{i=1}^{4} \lambda_i w_{iLA} \\
&= \lambda_{Seattle} w_{Seattle-LA} + \lambda_{SF} w_{SF-LA} + \lambda_{LA} w_{LA-LA} + \lambda_{Denver} w_{Denver-LA} \\
&= \lambda_{Seattle} 0.4 + \lambda_{SF} 0.6 + \lambda_{LA} 0 + \lambda_{Denver} 0 \\
&= \lambda_{Seattle} 0.4 + \lambda_{SF} 0.6
\end{aligned}$$

$$\begin{aligned}
\lambda_{Denver} &= \sum_{i=1}^{4} \lambda_{iDenver} = \sum_{i=1}^{4} \lambda_i w_{iDenver} \\
&= \lambda_{Seattle} w_{Seattle-Denver} + \lambda_{SF} w_{SF-Denver} + \lambda_{LA} w_{LA-Denver} + \lambda_{Denver} w_{Denver-Denver} \\
&= \lambda_{Seattle} 0.4 + \lambda_{SF} 0.3 + \lambda_{LA} 0.3 + \lambda_{Denver} 0 \\
&= \lambda_{Seattle} 0.4 + \lambda_{SF} 0.3 + \lambda_{LA} 0.3
\end{aligned}$$

To complete the network model, the flow rates satisfy the following constraints

1)$\lambda_{ij} = \lambda_{ji}$.

2)$\sum_i \lambda_{ij} = \sum_k \lambda_{jk}$. This states that sum of inflow to node j is equal to outflow from j as shown in figure 3.3.

For the example shown in figure 3.3, the second condition can be stated as $\lambda_{1j} + \lambda_{2j} = \lambda_{j2} + \lambda_{j3} + \lambda_{j4}$

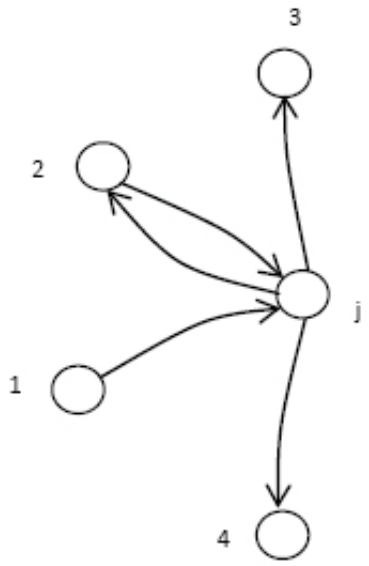

Figure 3.3. sum of inflow = sum of outflow

Thus, the network model with flow interactions was modelled successfully. In the next chapter, the mathematical formulation of the optimal long-term planning problem is discussed in detail.

3.4. Mathematical Formulaton of the Long-Term Investment Problem

Here, the long term planning problem is mathematically formulated for minimizing the total delay in the NAS over a period of time with limited capacity delivery costs. The section 3.4.1 provides an overview of the formulation of a general optimization problem, and section 3.4.2 provides the mathematical description of the optimal planning problem and an example that shows the use of the model for comparison of different planning schemes.

3.4.1. A General Study on the Formulation of Optimization Problems

Optimization refers to either maximing or minimizing an objective function to find the optimal values. The stationary points can be potential optimal solutions, however in most cases, the objective function is subject to some conditions which are known as constraints. The boundary points that hit the constraints can also be the optimal solutions.

Consider an example to solve the following optimization problem:

$$\text{minimize } \tfrac{w^2}{2} \text{ subject to } wx - 1 \geq 0$$

Here the objective function $\frac{w^2}{2}$ has to be minimized subject to the inequality constraint $wx - 1 \geq 0$. Suppose if the constraint doesn't exist, then the minimum value of $\frac{w^2}{2}$ exists at $w = 0$. But due to the presence of the constraint, the minimum value should also satisfy the constrained condition. In this case, subsituting $w = 0$ for $wx - 1 \geq 0$ doesn't satisfy the condition. Hence, the constraint should also be taken into account while optimizing the objective function.

3.4.2. Problem Formulation and an Example

The total delay for an airport j can be calculated as (refer to section 6.2)

$$\begin{aligned} D_j &= \frac{1 + \frac{var[S_j]}{E^2[S_j]}}{2} \frac{\lambda_j E[S_j]}{2(1 - \lambda_j E[S_j])} E[S_j] \\ &= \frac{\lambda_j E^2[S_j] + \lambda_j var[S_j]}{2(1 - \lambda_j E[S_j])} \end{aligned}$$

As backlog $B{=}D \times \lambda$, it implies

$$B_j = \frac{{\lambda_j}^2 E^2[S_j] + {\lambda_j}^2 var[S_j]}{2(1 - \lambda_j E[S_j])}$$

Consider the system to be modeled over a period of time(k), where $k = t_a$ to t_b, then the total backlog is

$$B_{total} = \sum_{k=t_a}^{t_b} \sum_{j=1}^{n} \frac{[\lambda_j(k)]^2 E^2[S_j(k)] + [\lambda_j(k)]^2 var[S_j(k)]}{2(1 - \lambda_j(k) E[S_j(k)])}$$

where $\lambda_j(k) = \sum_{i=1}^{n} \lambda_{ij}(k) = \sum_{i=1}^{n} [\lambda_i(k)] w_{ij}(k)$, λ_{ij} satisfies 1) $\lambda_{ij} = \lambda_{ji}$, 2) $\sum_i \lambda_{ij} = \sum_k \lambda_{jk}$, and $w_{ij}(k)$ is the weighted average. $\lambda_j(k)$ can be found using forecasted reports such as terminal area forecasts (TAF) [28].

Constraint The constraint related to this optimization problem is the limited money allocated during a period of time. The capacity delivery costs associated with the capacity increase should not exceed the allocated money. Thus, the optimization problem is defined as

$$\sum_{k=t_a}^{t_b}\sum_{j=1}^{n}[S_j(k)-S_j(k-1)] \leq \frac{limited\ money}{cost\ of\ unit\ capacity\ increase}$$

Optimization of the total backlog in the network over a period of time with respect to the constraint using optimization techniques may tell us where, when, and how much to increase the capacity, and gives the best NAS performance.

Now let me illustrate through an example that the network model allows the comparison of different planning strategies. Consider increasing the capacity for an allocated investment during a period of 7 years. Consider a network of 4 airport nodes (e.g. SFO, SAN, PHX, and DFW), and consider two management strategies for increasing the capacity in all of the four airport nodes. Then the backlog associated with each management strategy is plotted. The strategies for increasing the capacities are: 1) installing or upgrading navigation tools and software, and 2) building new runways.

Initially at time period year $k = 0$, the flow rates are
$\lambda_{SFO} = 44$, $\lambda_{SAN} = 43$, $\lambda_{PHX} = 46$, and $\lambda_{DFW} = 50$.
the capacities are $\mu_{SFO} = 70$, $\mu_{SAN} = 65$, $\mu_{PHX} = 75$, and $\mu_{DFW} = 80$.
(the measured units used in this example for flow rate and capacity are flights/hr)

$$W = \begin{bmatrix} w_{SFO-SFO} & w_{SFO-SAN} & w_{SFO-PHX} & w_{SFO-DFW} \\ w_{SAN-SFO} & w_{SAN-SAN} & w_{SAN-PHX} & w_{SAN-DFW} \\ w_{PHX-SFO} & w_{PHX-SAN} & w_{PHX-PHX} & w_{PHX-DFW} \\ w_{DFW-SFO} & w_{DFW-SAN} & w_{DFW-PHX} & w_{DFW-DFW} \end{bmatrix}$$

$$= \begin{bmatrix} 0 & 0.4 & 0.5 & 0.1 \\ 0.1 & 0 & 0.1 & 0.8 \\ 0.5 & 0.255 & 0 & 0.245 \\ 0.334 & 0.271 & 0.395 & 0 \end{bmatrix}$$

At year $k = 1$, $\lambda_{SFO} = 46$, $\lambda_{SAN} = 44$, $\lambda_{PHX} = 48$, and $\lambda_{DFW} = 51$.

$$W = \begin{bmatrix} 0 & 0.4 & 0.5 & 0.1 \\ 0.115 & 0 & 0.1 & 0.785 \\ 0.5 & 0.255 & 0 & 0.245 \\ 0.334 & 0.261 & 0.405 & 0 \end{bmatrix}$$

At year $k = 2$, $\lambda_{SFO} = 47$, $\lambda_{SAN} = 46$, $\lambda_{PHX} = 50$, and $\lambda_{DFW} = 53$.

$$W = \begin{bmatrix} 0 & 0.4 & 0.5 & 0.1 \\ 0.115 & 0 & 0.1 & 0.785 \\ 0.5 & 0.255 & 0 & 0.245 \\ 0.314 & 0.271 & 0.415 & 0 \end{bmatrix}$$

At year $k = 3$, $\lambda_{SFO} = 48$, $\lambda_{SAN} = 47$, $\lambda_{PHX} = 51$, and $\lambda_{DFW} = 54$.

$$W = \begin{bmatrix} 0 & 0.4 & 0.5 & 0.1 \\ 0.115 & 0 & 0.1 & 0.785 \\ 0.5 & 0.26 & 0 & 0.24 \\ 0.314 & 0.271 & 0.415 & 0 \end{bmatrix}$$

At year $k = 4$, $\lambda_{SFO} = 50$, $\lambda_{SAN} = 48$, $\lambda_{PHX} = 52$, and $\lambda_{DFW} = 55$.

$$W = \begin{bmatrix} 0 & 0.4 & 0.5 & 0.1 \\ 0.115 & 0 & 0.1 & 0.785 \\ 0.5 & 0.26 & 0 & 0.24 \\ 0.334 & 0.261 & 0.405 & 0 \end{bmatrix}$$

At year $k = 5$, $\lambda_{SFO} = 51$, $\lambda_{SAN} = 50$, $\lambda_{PHX} = 52$, and $\lambda_{DFW} = 55$.

$$W = \begin{bmatrix} 0 & 0.4 & 0.5 & 0.1 \\ 0.133 & 0 & 0.096 & 0.771 \\ 0.5 & 0.281 & 0 & 0.219 \\ 0.334 & 0.271 & 0.395 & 0 \end{bmatrix}$$

At year $k = 6$, $\lambda_{SFO} = 52$, $\lambda_{SAN} = 50$, $\lambda_{PHX} = 53$, and $\lambda_{DFW} = 56$.

$$W = \begin{bmatrix} 0 & 0.4 & 0.5 & 0.1 \\ 0.135 & 0 & 0.1 & 0.765 \\ 0.5 & 0.265 & 0 & 0.235 \\ 0.335 & 0.271 & 0.393 & 0 \end{bmatrix}$$

At year $k = 7$, $\lambda_{SFO} = 54$, $\lambda_{SAN} = 52$, $\lambda_{PHX} = 54$, and $\lambda_{DFW} = 57$.

$$W = \begin{bmatrix} 0 & 0.4 & 0.5 & 0.1 \\ 0.14 & 0 & 0.132 & 0.728 \\ 0.5 & 0.246 & 0 & 0.254 \\ 0.346 & 0.3 & 0.353 & 0 \end{bmatrix}$$

At year $k = 8$, $\lambda_{SFO} = 56$, $\lambda_{SAN} = 53$, $\lambda_{PHX} = 54$, and $\lambda_{DFW} = 58$.

$$W = \begin{bmatrix} 0 & 0.4 & 0.5 & 0.1 \\ 0.15 & 0 & 0.122 & 0.728 \\ 0.5 & 0.244 & 0 & 0.256 \\ 0.363 & 0.3 & 0.336 & 0 \end{bmatrix}$$

Strategy 1: Increasing the capacity with navigation tools (figure 3.4a).

for $k = 1$, $\mu_{SFO} = 71.125$, $\mu_{SAN} = 66.125$, $\mu_{PHX} = 76.125$, and $\mu_{DFW} = 81.125$.

for $k = 2$, $\mu_{SFO} = 72.25$, $\mu_{SAN} = 67.25$, $\mu_{PHX} = 77.25$, and $\mu_{DFW} = 82.25$.

for $k = 3$, $\mu_{SFO} = 73.375$, $\mu_{SAN} = 68.375$, $\mu_{PHX} = 78.375$, and $\mu_{DFW} = 83.375$.

for $k = 4$, $\mu_{SFO} = 74.5$, $\mu_{SAN} = 69.5$, $\mu_{PHX} = 79.5$, and $\mu_{DFW} = 84.5$.

for $k = 5$, $\mu_{SFO} = 75.625$, $\mu_{SAN} = 70.625$, $\mu_{PHX} = 80.625$, and $\mu_{DFW} = 85.625$.

for $k = 6$, $\mu_{SFO} = 76.75$, $\mu_{SAN} = 71.75$, $\mu_{PHX} = 81.75$, and $\mu_{DFW} = 86.75$.

for $k = 7$, $\mu_{SFO} = 77.875$, $\mu_{SAN} = 72.875$, $\mu_{PHX} = 82.875$, and $\mu_{DFW} = 87.875$.

Strategy 2: Increasing the capacity by building new runway (figure 3.4b).

for $k = 1, 2, 3$,$\mu_{SFO} = 70$, $\mu_{SAN} = 65$, $\mu_{PHX} = 75$, and $\mu_{DFW} = 80$.

for $k = 5, 6, 7$,$\mu_{SFO} = 85$, $\mu_{SAN} = 80$, $\mu_{PHX} = 90$, and $\mu_{DFW} = 95$.

As the backlog equation can be calculated as

$$B_j(k) = \sum_{k=t_a}^{t_b} \sum_{j=1}^{n} \frac{[\lambda_j(k)]^2 E^2[S_j(k)] + [\lambda_j(k)]^2 var[S_j(k)]}{2(1 - \lambda_j(k) E[S_j(k)])}$$

where $\lambda_j(k) = \sum_{i=1}^{n} \lambda_{ij}(k) = \sum_{i=1}^{n} [\lambda_i(k)] w_{ij}(k)$

Applying to the proposed network model with 4 nodes and time period of 7 years, the total delay can be found as

$$Total = \sum_{k=0}^{7} \sum_{j=1}^{4} \frac{[\lambda_j(k)]^2 E^2[S_j(k)] + [\lambda_j(k)]^2 var[S_j(k)]}{2(1 - \lambda_j(k) E[S_j(k)])}$$

Substituting the above values for $\lambda_j(k)$, and $E[S_j(k)] = \frac{1}{\mu_j(k)}$ for each of the two management strategies, the total backlog for a period of 7 years ares plotted in figure 3.5.

Consider the behavior for the time period of 3 years; the number of delayed flights is less for the management strategy that increases capacity with navigation tools. For the time period of 7 years, the number of delayed flights in the network is less for the management strategy that increases capacity by building a new runway. These results state that in order to maximize the performance in a network, increasing the capacity with navigation tools or software updates yields less delays for a shorter time period, and constructing new runways yield less delays for a longer time period with limited allocated money.

3.4.3. Future Work

The preliminary network model presented in this thesis considers minimizing the total delay in the NAS. The network model needs to further reflect the complicated correlation between delay and demand, and also needs to consider more realistic optimization goal functions. Further the optimization solution has to be developed that answers where, when, and how much to increase the capacity.

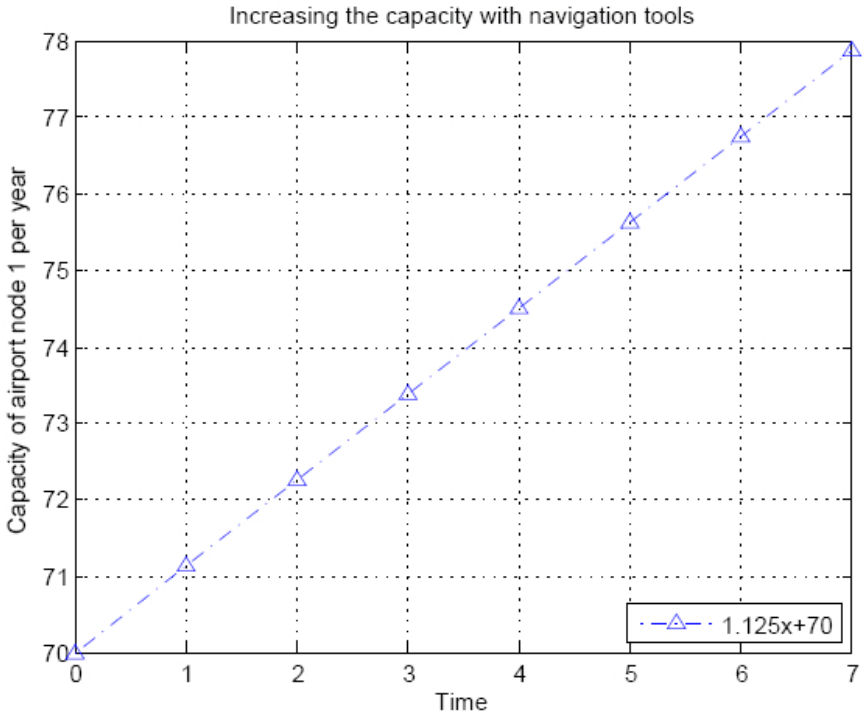

(a) Increasing the capacity with navigation tools

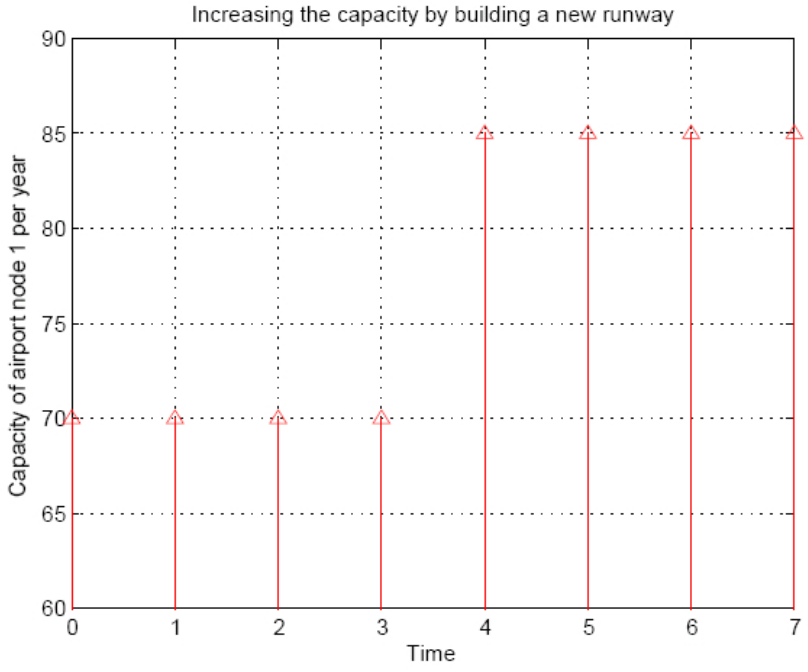

(b) Increasing the capacity by building new runway

Figure 3.4. Implemetation of two management strategies for increasing the capacity over a period of 7 years

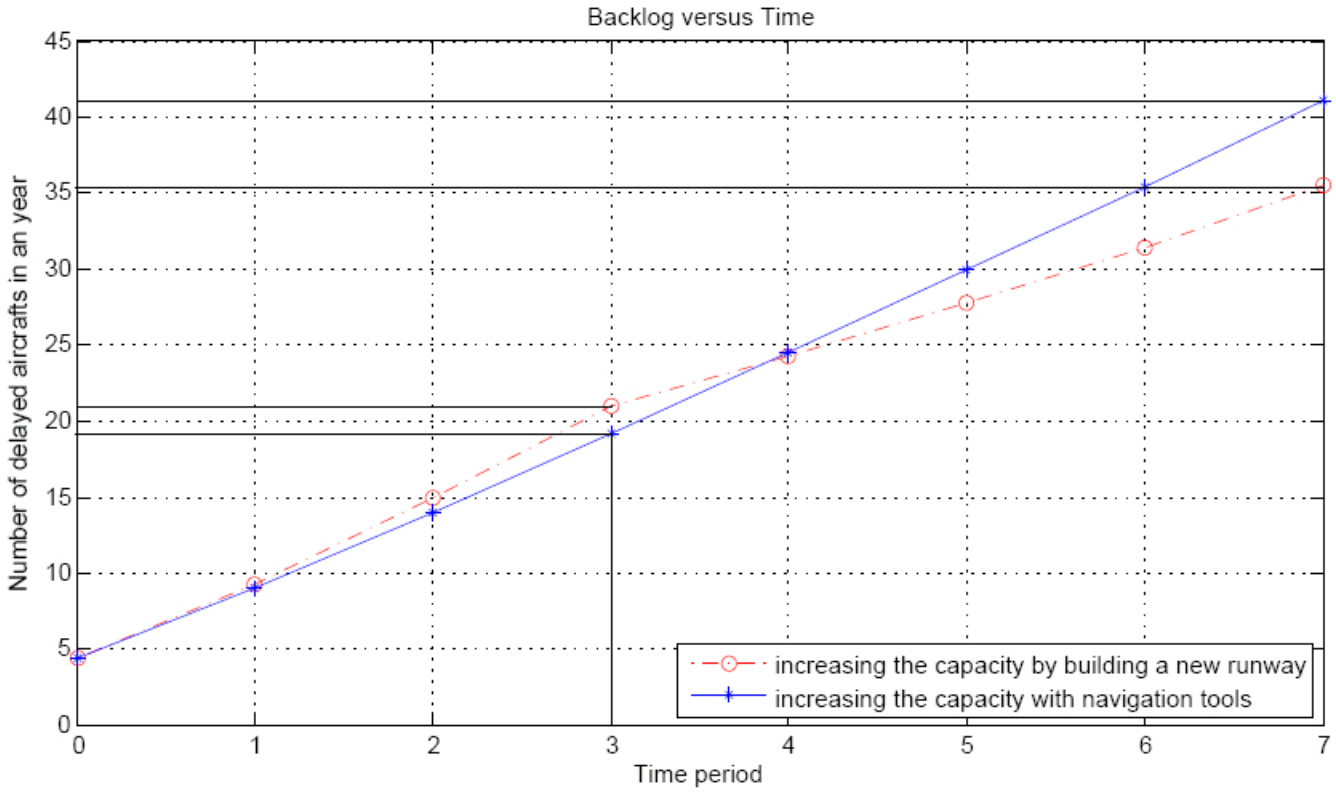

Figure 3.5. Number of flights delayed upon implementation of two management strategies

CHAPTER 4

CONCLUSION

Problems in both parts were formulated as network models where the structure impacts the performance. In the consensus building problem (Part I), the multi-group network structure is related to the convergence behavior of consensus building strategies. The structure is captured using a routing matrix H, and inferring eigenvalues directly from the struture leads to design of a DSN that meets desired performance. In long term planning of NAS (Part II), the network structure in the NAS is captured using a weighted average matrix W which allows to calculate the backlog. This backlog is minimized with respect to constraints to maximize the performance in the NAS over a period of time.

Specifically, in the consensus problem in multi-group structures, the structure and dynamics are related using eigen-analysis where the stability and performance of the system are known. The inference of eigenvalues from the structure provides an interesting approach to expose hidden graph structures that are not possible otherwise. The approach to consensus analysis and design given in this thesis can be extended to other iterative consensus algorithms, and DSNs described by graphs other than tanner graphs, e.g., hierarchical graphs.

In long term planning of the NAS, considering the complexity in NAS, the planning problem is formulated as resource allocation problem for a flow network. A preliminary network model is considered with flows transitting among airports, and optimization problem is formulated which is aimed to minimize the total delay in the NAS over a time span with limited infrastructure delivery costs. An example is illustrated in which the proposed model is used for comparison of different planning schemes. The results provided that in order to maximize the performance in a network, inceasing the capacity with navigation tools or software updates yield less delays for

a shorter time period, and constructing new runways yield less delays for a longer time period with limited allocated money. The network model needs to further reflect the complicated correlation between delay and demand, and also needs to consider more realistic optimization goal functions. Further the optimization solution has to be developed that answers where, when, and how much to increase the capacity.

BIBLIOGRAPHY

[1] S. Tarannum and S. Srividya and D. S. Asha and R. Padmini and L. Nalini and K. R. Venugopal and L.M. Patnaik, "Dynamic hierarchical communication paradigm for wireless sensor networks: a centralized, energy effient approach", *11th IEEE Singapore International Conference on Communication Systems.*, pp. 959-963, March, 2008.

[2] Y. Wan and K. Namuduri and S. Akula and M. Varanasi, "Consensus Building in Distributed Sensor Networks with Bipartite Graph Structures", *submitted to International Journal of Robust and Nonlinear Control*, 2010.

[3] M. Shukair and K. Namuduri, "LDPC-like belief propagation algorithm for consensus building in wireless sensor network", *43rd Annual Conference on Information Sciences and Systems*, pp. 805-810, 2009.

[4] R. G. Gallager, "Discrete Stochastic Processes", Kluwer Academic Publishers, 1996.

[5] http://en.wikipedia.org/wiki/Spectral radius.

[6] V. Quera and F. S. Beltran and R. Dolado, "Flocking behaviour: agent-based simulation and hierarchical leadership", *Report, Wireless Sensor Network*, November, 2009.

[7] R. M. Tanner, "A Recursive Approach to Low Complexity Codes", *IEEE Transactions on Information Theory*, vol.27, pp. 533-547, September, 1981.

[8] F. R. K. Chung, "Spectral graph theory", American Mathematical Society, 1997.

[9] L. Xiao and S. Boyd, "Fast Linear Iterations for Distributed Averaging", *Proc. 42nd IEEE Conf. on Decision and Control*, vol.5, pp. 4997-5002, December, 2003.

[10] S. Boyd and P. Diaconis and L. Xiao, "Fast Mixing Markov Chain on a Graph", *SIAM Review*, vol.46, pp. 667-689, 2004.

[11] S. Boyd and A. Ghosh and B. Prabhakar and D. Shah, "Randomized Gossip Algorithms", *IEEE Transactions on Information Theory*, vol.52, pp. 2508-2530, June, 2006.

[12] C. W. Wu and L. O. Chua, "Application of Kronecker Products to the Analysis of Systems with Uniform Linear Coupling", *IEEE Transaction on Circuit and Systems I*, vol.42, pp. 775-779, October, 1995.

[13] W. Ren and R. W. Beard and E. A. Atkins, "Information Consensus in Multivehicle Cooperative Control", *IEEE Control Systems Magazine*, vol.27, pp. 71-82, April, 2007.

[14] S. Roy and A. Saberi and K. Herlugson, "A control-theoretic perspective on the design of agreement protocol", *International Journal of Robust and Nonlinear Control*, vol.17, pp. 1034-1066, December, 2006.

[15] S. Roy and A. Saberi and K. Herlugson, "A control-theoretic perspective on the design of agreement protocol", *International Journal of Robust and Nonlinear Control*, vol.17, pp. 1034-1066, December, 2006.

[16] N. A. Lynch, "Distributed Algorithms", Springer, 1996.

[17] J. Kelner, "An Algorithm's Toolkit", 2009.

[18] S. Roy and Y. Wan and A. Saberi and M. Xue, "Designing linear distributed algorithms with memory for fast convergence", *48th IEEE Conference on Decision and Control*, pp. 7080-7085, December, 2009.

[19] R. G. Gallager, "Low-Density Parity-Check Codes", *MIT Press*, 1963.

[20] M. Fiedler, "Absolute algebraic connectivity of trees", *Linear and Multilinear Algebra*, vol.423, pp. 53-73, May, 2007.

[21] Y. Wan and S. Roy and X. Wang and A. Saberi and T. Yang and M. Xue and B. Malek, "On the structure of graph edge designs that optimize the algebraic connectivity", *Proceedings of 47th IEEE Conference on Decision and Control*, pp. 805-810, December, 2008.

[22] Y. Wan and S. Roy and A. Saberi, "A new focus in the science of networks: towards methods for design", *Proceedings of the Royal Society A*, vol.464, pp. 513-535, March, 2008.

[23] S. Roy and A. Saberi and P. Petite, "Scaling: a canonical design problem for networks", *Proceedings of the 2006 American Control Conference*, pp. 5568-5575, June, 2006.

[24] C.Chong and S.P.Kumar, "Sensor networks:Evolution, opportunities, and challenges", *Proceedings of the IEEE*, vol.91, August, 2003.

[25] J.Yang and C.Zhang and X.Li and Y.Huang and S.Fu and M.acevedo, "Integration of wireless sensor networks in environmental monitoring cyber infrastructure", *Wireless Networks, Springer/ACM*, June, 2009.

[26] A. Tomer and R. Puentes, "Expected delays: An analysis of Air Travel Trends in the United States", *Metropolitan infrastructure initiative series*, October, 2009.

[27] United States Government Accountability Office (GAO), "NATIONAL AIRSPACE SYSTEM: Regional Airport Planning Could Help Address Congestion If Plans Were Integrated with FAA and Airport Decision Makings", December, 2009.

[28] Federal Aviation Administration, "Terminal Area Forecast Summary", 2009.

[29] J. F. Shortle and D. Gross and B. L.Markl, "Efficient Simulation Of The National Airspace System", *Proceedings of the 2003 Winter Simulation Conference*, pp. 441-448, 2003.

[30] Capacity Needs in the National Airspace System, "The MITRE Corporation, Center for Advanced Aviation System Development", May, 2007.

[31] M. D. Tandale and P. Sengupta and P. K. Menon and V. H.L. Cheng and J. Rosenberger and K. Subbarao, "Queueing Network Models of the National Airspace System", *The 26th Congress of International Council of the Aeronautical Sciences*, September, 2008.

[32] D. C. Moreau and S. Roy, "A Stochastic Characterization of En Route Traffic Flow Management Strategies", *presented at the AIAA Guidance, Navigation, and Control Conf., San Francisco, CA*, 2005.

[33] S. Roy and B. Sridhar and G. C. Verghese, "An aggregate dynamic stochastic model for an air traffic system", *in Proc. 5th Eurocontrol/Federal Aviation Agency Air Traffic Manage. Res. Dev. Semin., Budapest, Hungary*, June, 2003.

[34] Y. Wan and S. Roy, "A Scalable Methodology for Evaluating and Designing Coordinated Air-Traffic Flow Management Strategies Under Uncertainity", *IEEE Transactions on Intelligent Transportation Systems*, vol.9, pp. 644-656, December, 2008.

[35] B. Miller and J.P Clarke, "The hidden value of air transportation infrastructure", *Presented at the 7th International Conference on Technology Policy and Innovation in Monterrey, Mexico*, June, 2003.

[36] D. Gross and J. F.Shortle and J. M.Thompson and C. M.Harris, "Fundamentals of Queueing Theory", A John Wiley Sons, Inc., Publication, 2008.